Oceans — the sediment graveyard

So... what happens to all of this sediment after it arrives at the ocean ?

Recall total $2 \cdot 10^{10}$ tons of suspended sediment /year

Top 20 rivers deliver about 20% of this — remember this is the top 20 in order of H_2O not sediments.

At the mouth of every river there is a delta

Prototype — the Nile delta — name comes from resemblence to Greek letter Δ
Cradle of Egyptian civilization.

Niger River in Africa another classic Δ-shaped delta

Note size — about 100 km × 100 km

Ganges — Brahmaputra delta in Bangladesh is much larger 600 km × 600 km
Home to many people — fertile floodplain — fifth biggest river in terms of H_2O discharge — monsoon causes annual flooding — millions of people affected.

TABLE 5.2 Suspended Sediment Carried by Rivers to the Ocean (in Metric Tons)

Continent	Drainage Area Contributing Sediment to Ocean (10^6 km^2)	Sediment Discharge (10^6 tons/yr)	Sediment Yield (tons/km^2/yr)	Mean Continental Elevation (km)
North America	15.4	1020	66	0.72
Central America[a]	2.1	442	210	—
South America	17.9	1788	97	0.59
Europe	4.61	230	50	0.34
Eurasian Arctic	11.17	84	8	~0.2
Asia	16.88	6349	380	0.96
Africa	15.34	530	35	0.75
Australia	2.2	62	28	0.34
Pacific & Indian Ocean Islands[b]	3.0	9000[c]	3000[c]	~1.0
World total	88.6	20,000[d]	226[d]	

[a] Includes Mexico.

[b] Japan, Indonesia, Taiwan, Phillipines, New Guinea, and New Zealand (Oceania).

[c] From Milliman and Syvitski (1992).

[d] From Milliman and Syvitski (1992). Data reflect greater sediment discharge from South America, the Alps-Caucusus Mountains, and northwest Africa, in addition to Oceania.

Sources: After Milliman and Meade (1983) and Milliman and Syvitski (1992), elevations from Fairbridge (1968).

TABLE 5.1 Major Rivers that Flow to the Sea, Listed in Order of Discharge

		Annual Discharge				
River	Location	Water (km^3/yr)	Dissolved Solids (Tg/yr)	Suspended Solids (Tg/yr)	Dissolved/ Suspended Ratio	Drainage Area (10^6 km^2)
1. Amazon	S. America	6300	275	1200	0.23	6.15
2. Zaire (Congo)	Africa	1250	41	43	0.95	3.82
3. Orinoco	S. America	1100	32	150	0.21	0.99
4. Yangtze (Chiang)	Asia (China)	900	247	478	0.53	1.94
5. Brahmaputra	Asia	603	61	540	0.11	0.58
6. Mississippi	N. America	580	125	210 (400)	0.60	3.27
7. Yenisei	Asia (Russia)	560	68	13	5.2	2.58
8. Lena	Asia (Russia)	525	49	18	2.7	2.49
9. Mekong	Asia (Vietnam)	470	57	160	0.36	0.79
10. Ganges	Asia	450	75	520	0.14	0.975
11. St. Lawrence	N. America	447	45	4	11.3	1.03
12. Parana	S. America	429	16	79	0.20	2.6
13. Irrawaddy	Asia (Burma)	428	92	265	0.35	0.43
15. Mackenzie	N. America	306	64	42	1.5	1.81
17. Columbia	N. America	251	35	10 (15)	3.5	0.67
20. Indus	Asia (India)	238	79	59 (250)	1.3	0.975
Red (Hungho)	Asia (Vietnam)	123	?	130	?	0.12
Huanghe (Yellow)	Asia (China)	59	22	1100	0.02	0.77

Note: Tributaries are excluded. Tg = 10^6 tons = 10^{12} g.

Sources: Water and suspended solids from Milliman and Meade (1983) and Milliman and Syvitski (1992). Dissolved solids calculated from Table 5.7 and Pinet and Souriau (1988) (for the Irrawaddy). Suspended load values in parentheses indicate pre-dam values.

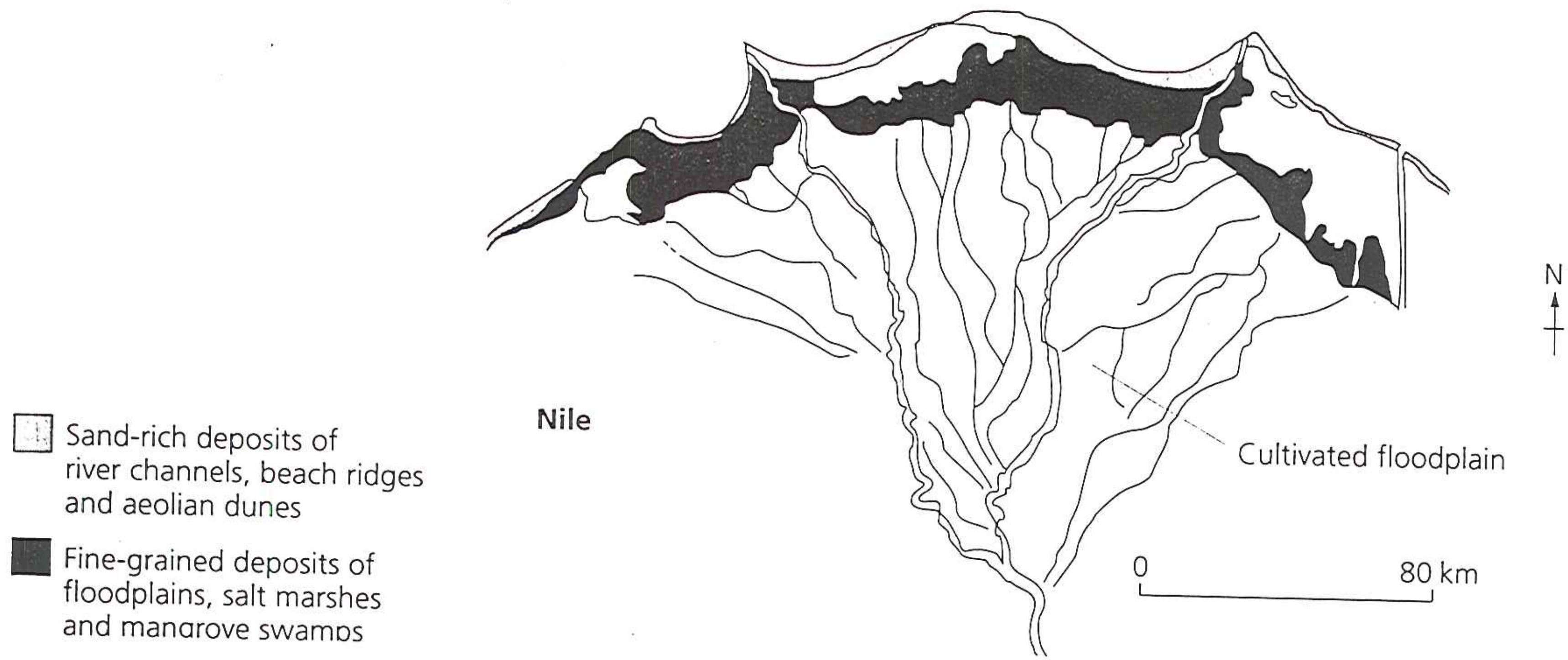

Fig. 7.14 *See p. 262 for caption.*

FIGURE 14.35 In this picture taken from Gemini 4 the Nile Delta is prominent because its well-vegetated surface stands out in contrast to the neighboring desert. *(NASA)*

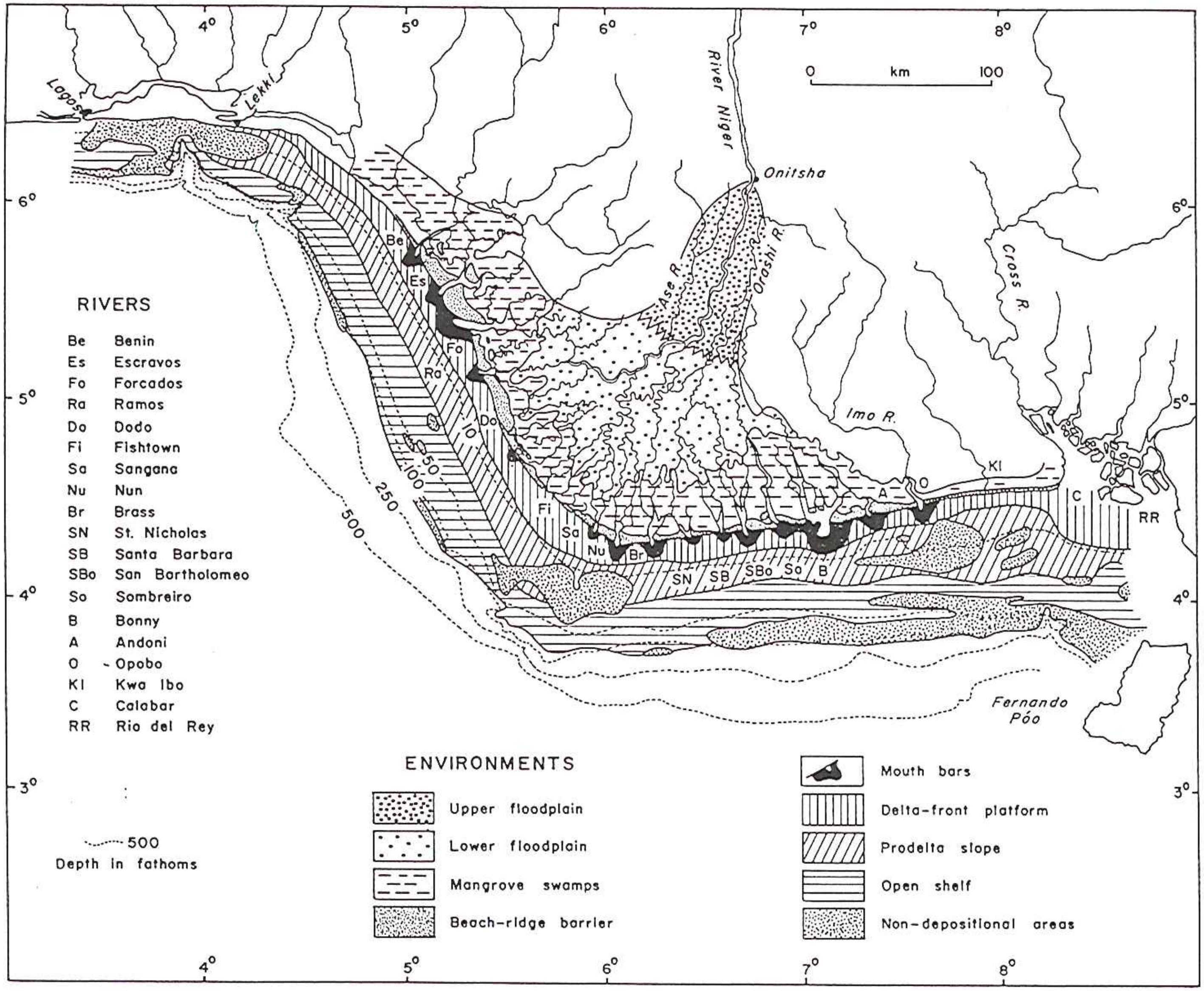

FIG. 2.—Principal sedimentary environments of the Niger delta.

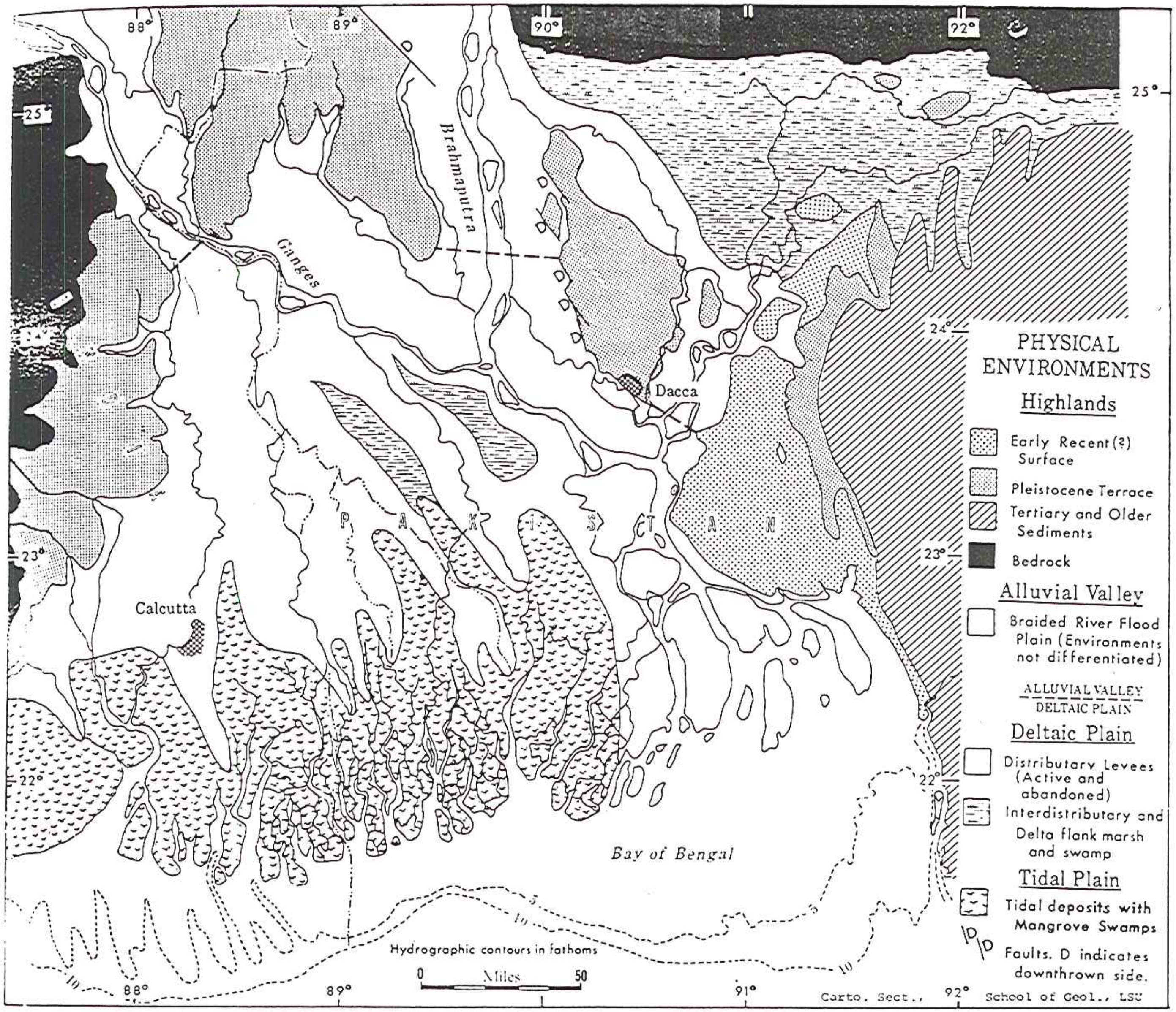

Fig. 6.—Depositional environments of the Ganges-Brahmaputra delta, East Pakistan and India.

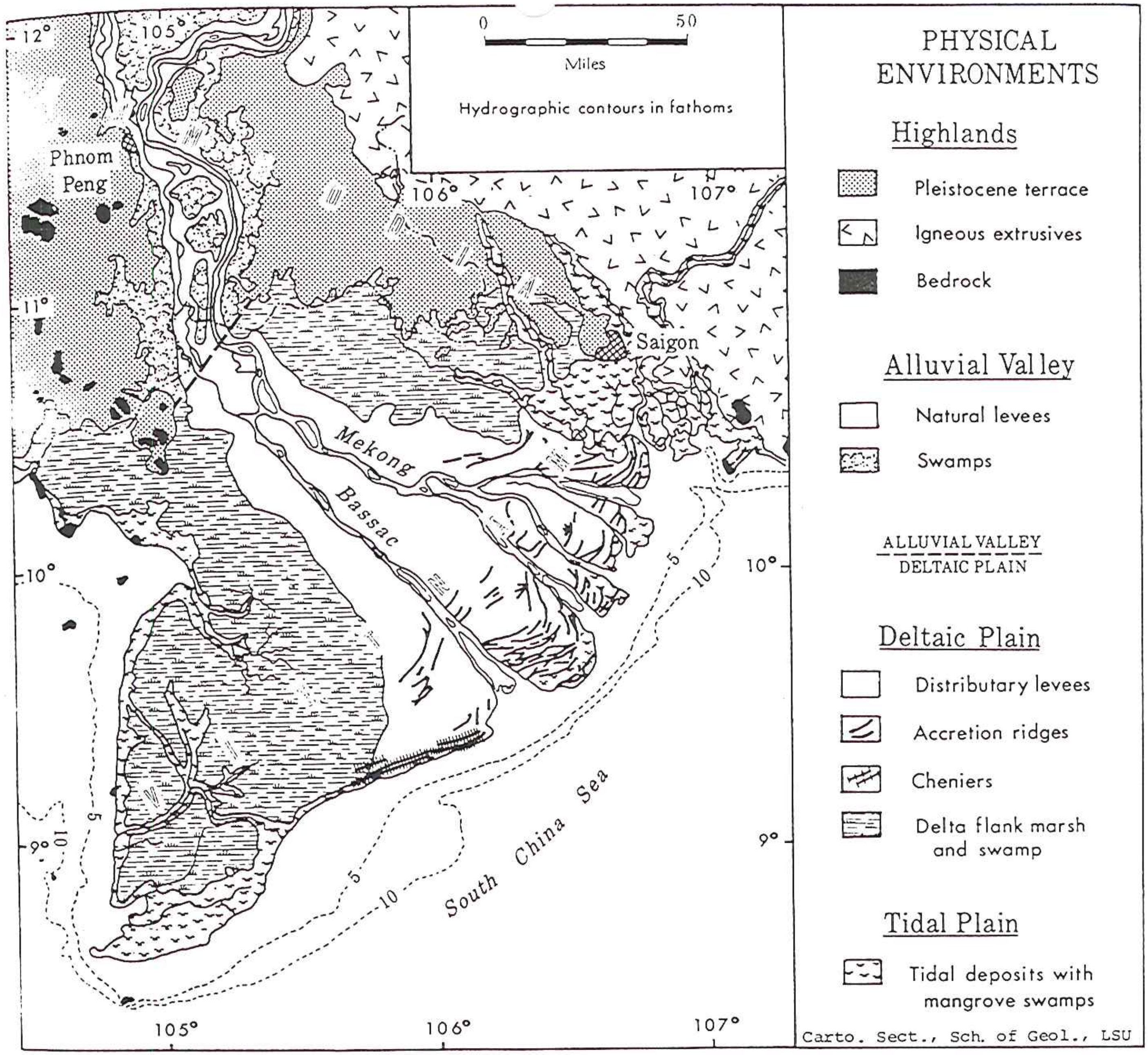

FIG. 11.—Depositional environments of the Mekong delta, Vietnam and Cambodia.

Also show Mekong River delta in Vietnam — 9th biggest river

Next show several transparencies of Mississippi River delta — more complicated morphology — a so-called birdfoot delta — 6th biggest river

4 main channels branch off from the Head of Passes:
SW, S, SE → N + NE

Note the natural levees that confine the flow within this channel.

In fact, this birdfoot delta is merely the present mouth of the Mississippi — larger map Fig. 8 shows many abandoned channels to the west — note the Atchafalaya River — currently accounts for ~ 25% of the total H_2O flow — only large-scale engineering efforts by US Army Corps of Engineers has prevented modern capture of the entire flow — economy of New Orleans very heavily dependent on the river.

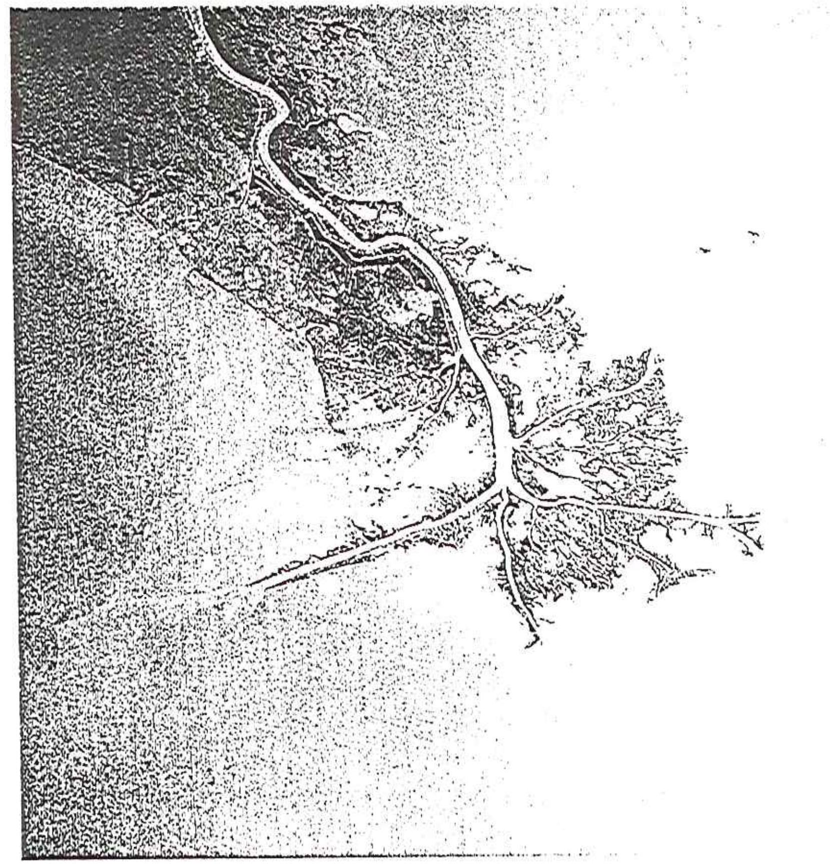

Plate 7.1 View of the delta formed by the River Mississippi as seen from Shuttle Challenger on mission 61A of 30 October to 6 November 1985. This photograph shows clearly the pattern of sediment deposition of this type of river delta. Between the kinks in the river towards the top left is the Town of Buras. From the tip of the Southwest Point (left) to North Point (right) is a distance of around 50 km. Photograph courtesy of the Science Photo Library, London; originally from the NASA/Science Photo Library, USA.

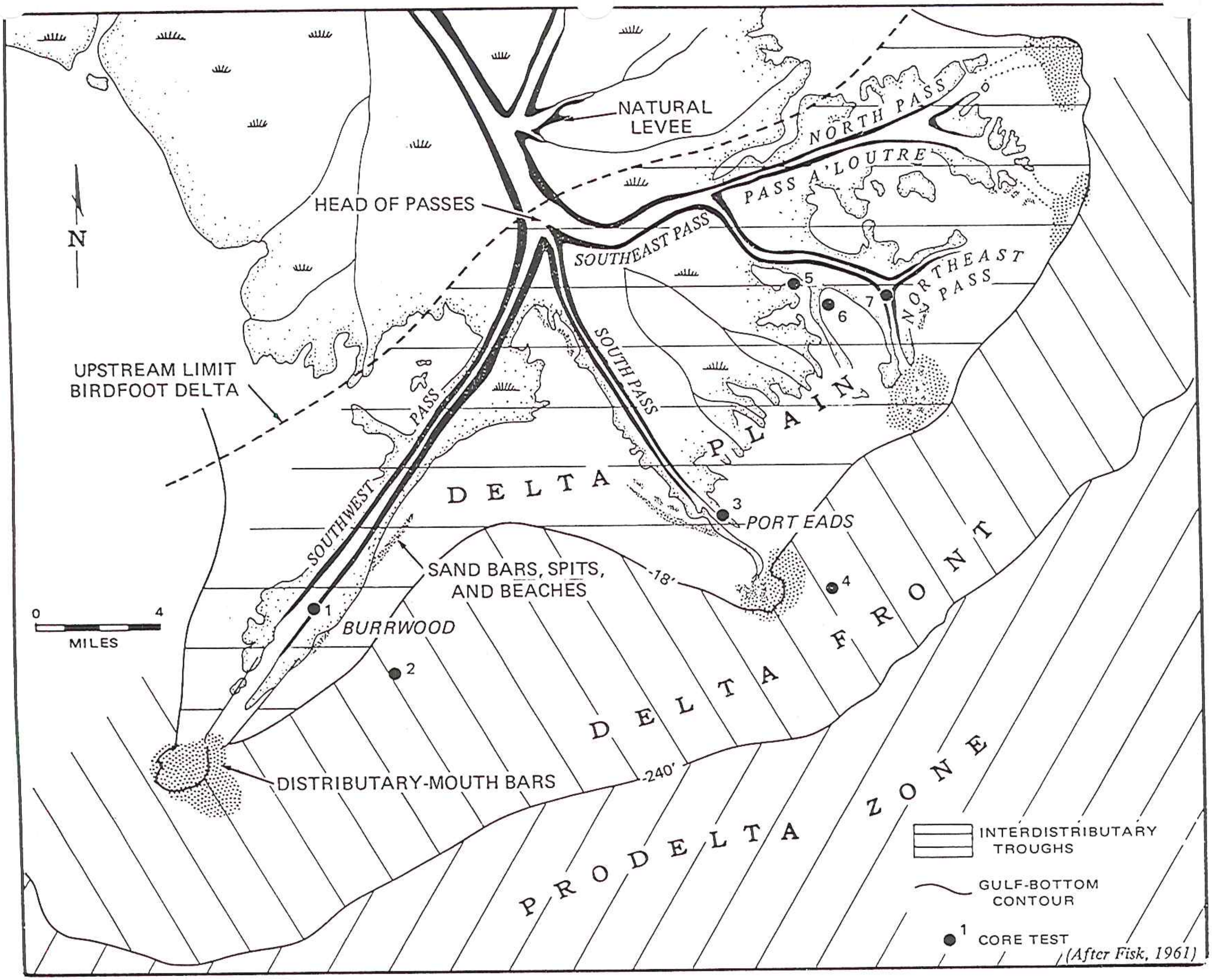

Fig. 17.—Depositional environments of Mississippi birdfoot delta.

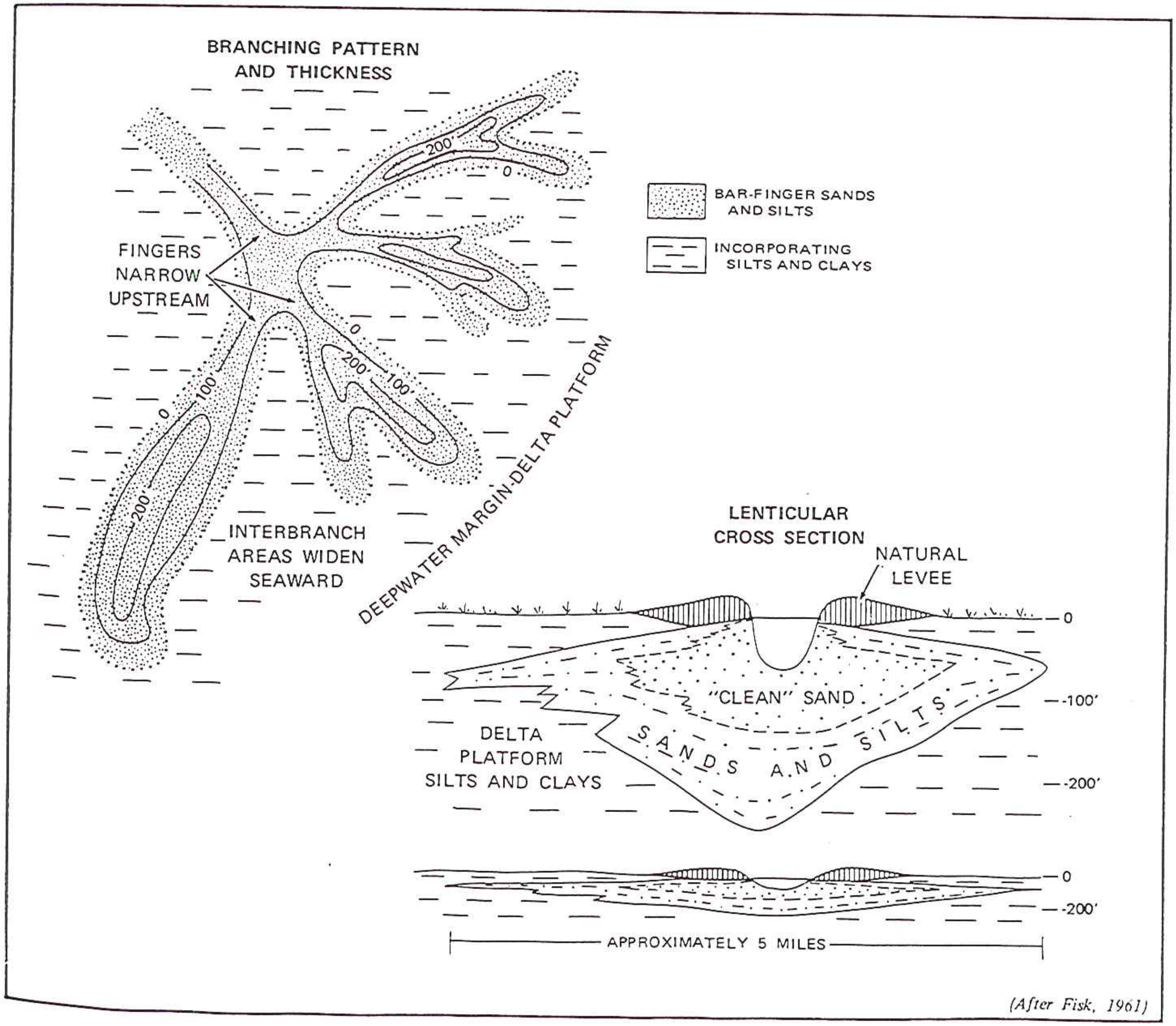

FIG. 25.—Distinguishing geometric and sedimentary characteristics of bar-finger sands.

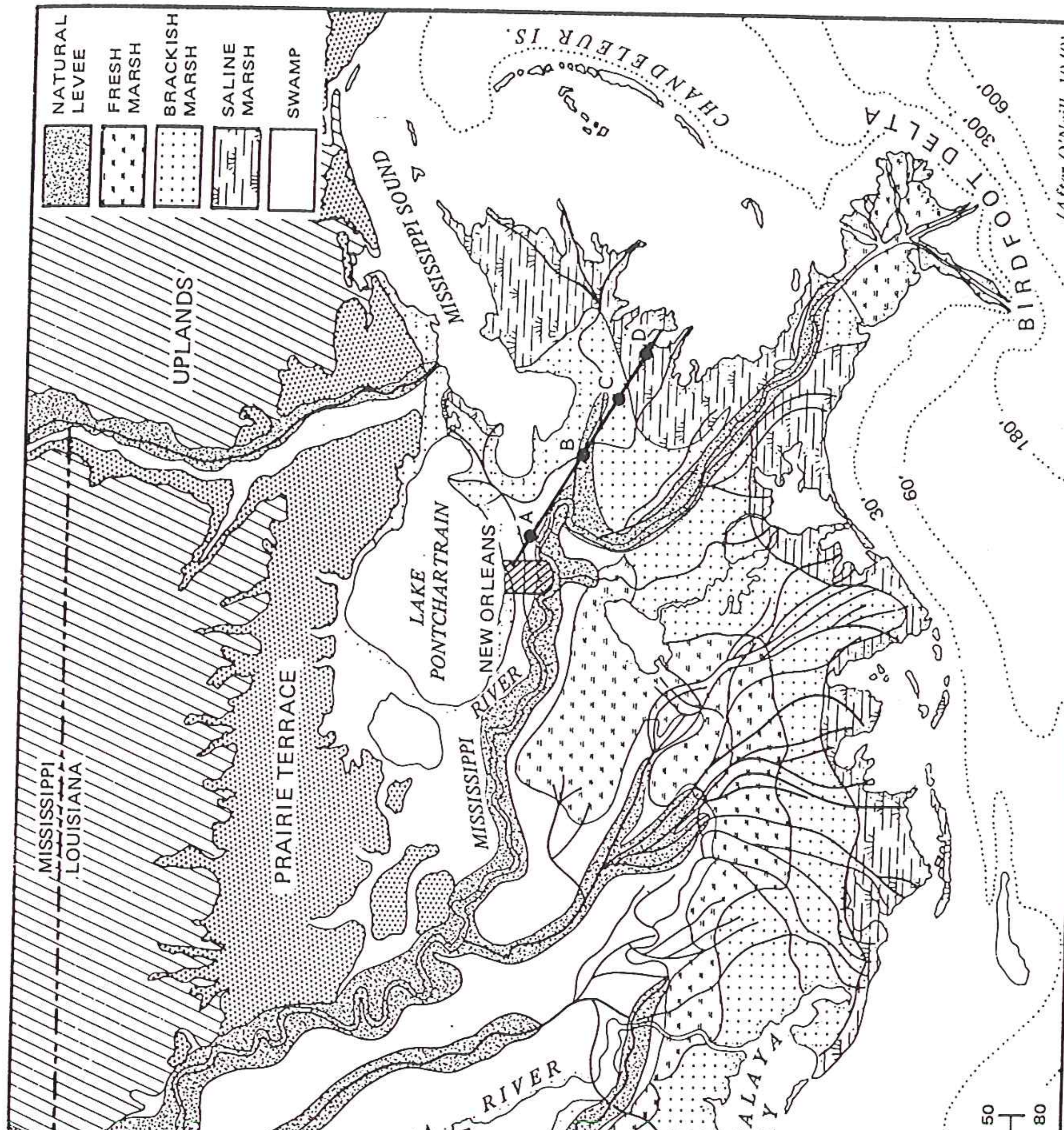

FIG. 8.—Distribution of swamp and marsh environments on Mississippi deltaic plain.

Fig. 7.9 shows salinity structure of flow near the mouth

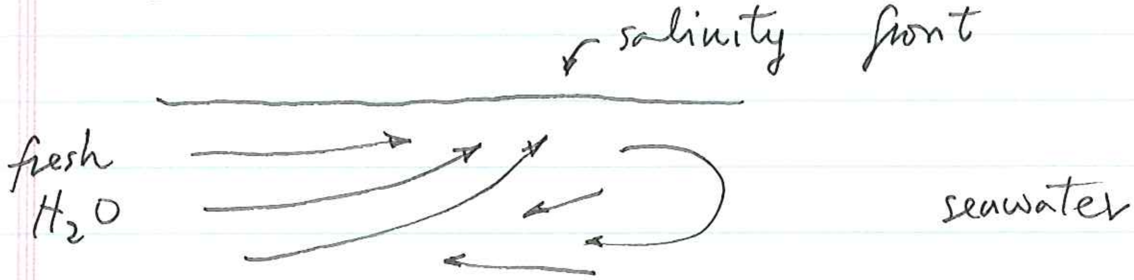

pycnocline = line of constant salinity

Froude number $= \dfrac{u}{\sqrt{\frac{\Delta\rho}{\rho} g h}}$

$(\Delta\rho/\rho)_{jump} \approx 2\%$
density of seawater
1035 kg/m^3

So, the jump of 1000 → 1020 across the salinity front is not to pure seawater — but more than half of mixing occurs here.

Fig. 7.6. from Berner shows that there is a turbidity maximum at this front — data from another smaller river (York, in VA)

Fig. 7.17 shows same phenomenon in Seine estuary — very common estuarine feature — much of the suspended sediment load is dumped at this salinity front. Two reasons:

- water is moving uphill over the salt wedge
- much more importantly, the ionic charge of the dissolved salt (Na^+, Ca^{2+}, Mg^{2+}, Cl^-) gives rise to a 'flocculation' or aggregation of the fine-grained clay — larger agglomerated particles sink out

The dropping of the sedimentary load gives rise to mouth bars at the mouths of all the channels — these shown as ∴∵ on map Fig. 17, and in cross-section Fig 7.10 — which also shows the flow during both a flooding & ebbing tide.

Fig. 20 shows the development with time of the Southwest Pass Bar Finger Position since 1764 is shown.

The delta is growing outward into the Gulf of Mexico at a rate

$$\frac{8 \text{ miles}}{200 \text{ years}} = \frac{70 \text{ km}}{1000 \text{ years}}$$ — migration rate of delta

↑ directly measured by historical surveys

The entire birdfoot has been built in ~ 1000 years

This gives an idea of the rapid dynamic nature of the sedimentation process.

see map showing previous delta locations going back ~ 5000 yrs.

In addition to sedimentation within the delta proper, the sediment flux from large rivers is deposited in <u>submarine fans</u> onto the adjacent deep ocean floor.

Analogous to the <u>alluvial fans</u> in desert environments

The mode of transport is via <u>turbidity currents</u> — Grand Banks cable break example

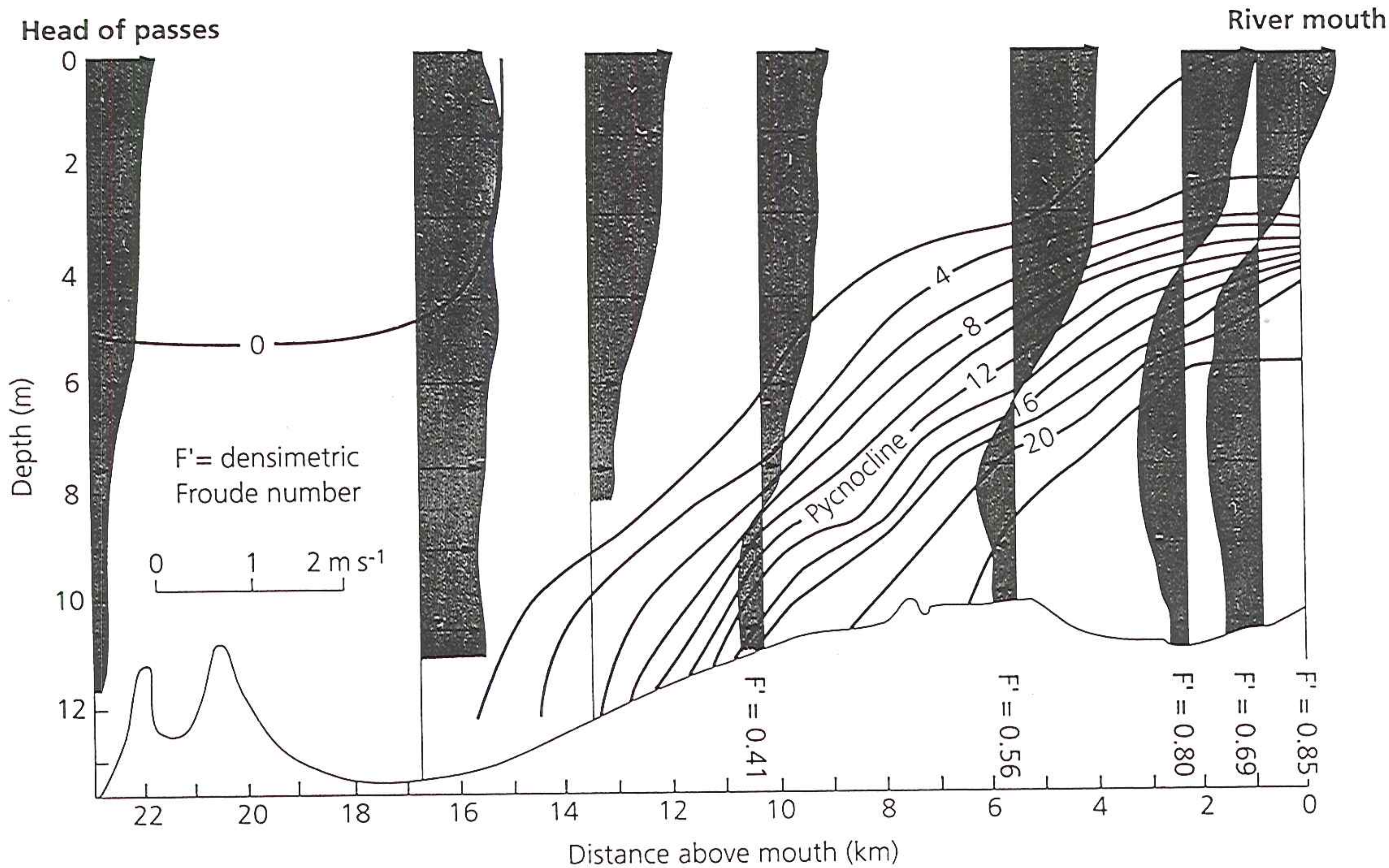

Fig. 7.9 Salinity structure (measured as density in excess of 1000 kg m^{-3}) and velocities between the South Pass river mouth and Head of Passes at a time of low to normal discharge. Densimetric Froude numbers are superimposed. At low stage the pycnocline is well developed between the overriding fresh water plume and the underlying salt wedge. After Wright & Coleman (1974) [4].

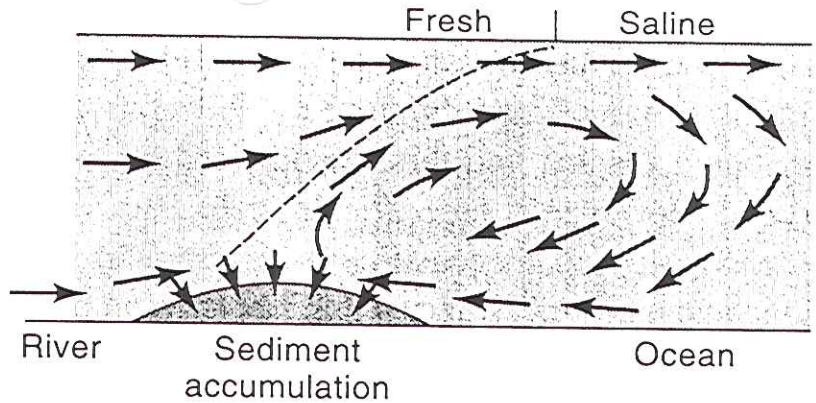

Figure 7.7. Suspended matter transport (arrows) and sediment accumulation near landward limit of sea-water mixing in an estuary. Dashed line is fresh–saline water boundary. (After Meade 1972.)

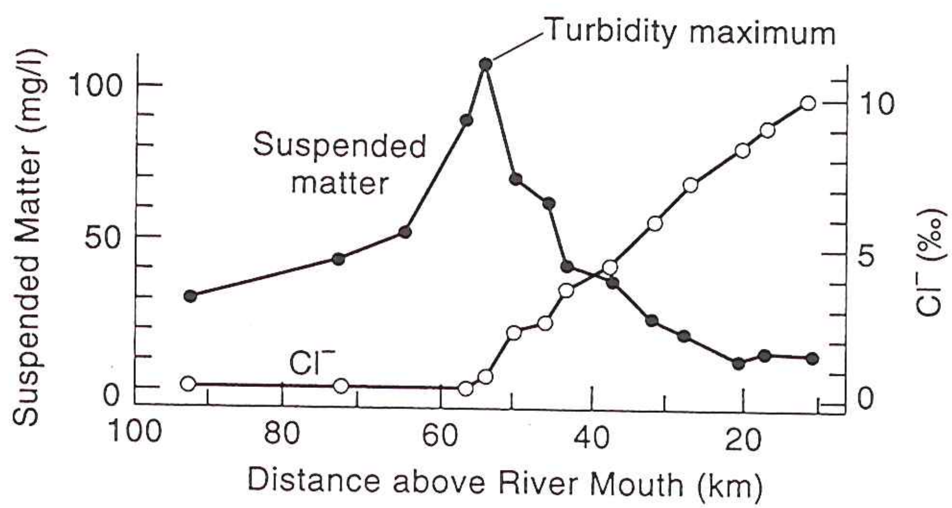

Figure 7.6. Concentration of suspended matter versus chlorinity in York River, Virginia, showing a *turbidity maximum* at the landward limit of sea-salt penetration into the estuary, e.g., where the chloride concentration drops to nearly zero. [After R. H. Meade, 1972, "Transport and Deposition of Sediment in Estuaries," *Geol. Soc. Am. Mem.* 133: 100; and B. N. Nelson, 1960, "Recent Sediment Studies in 1960," *Va. Polytech. Inst. J.* 7(4): 1–4.]

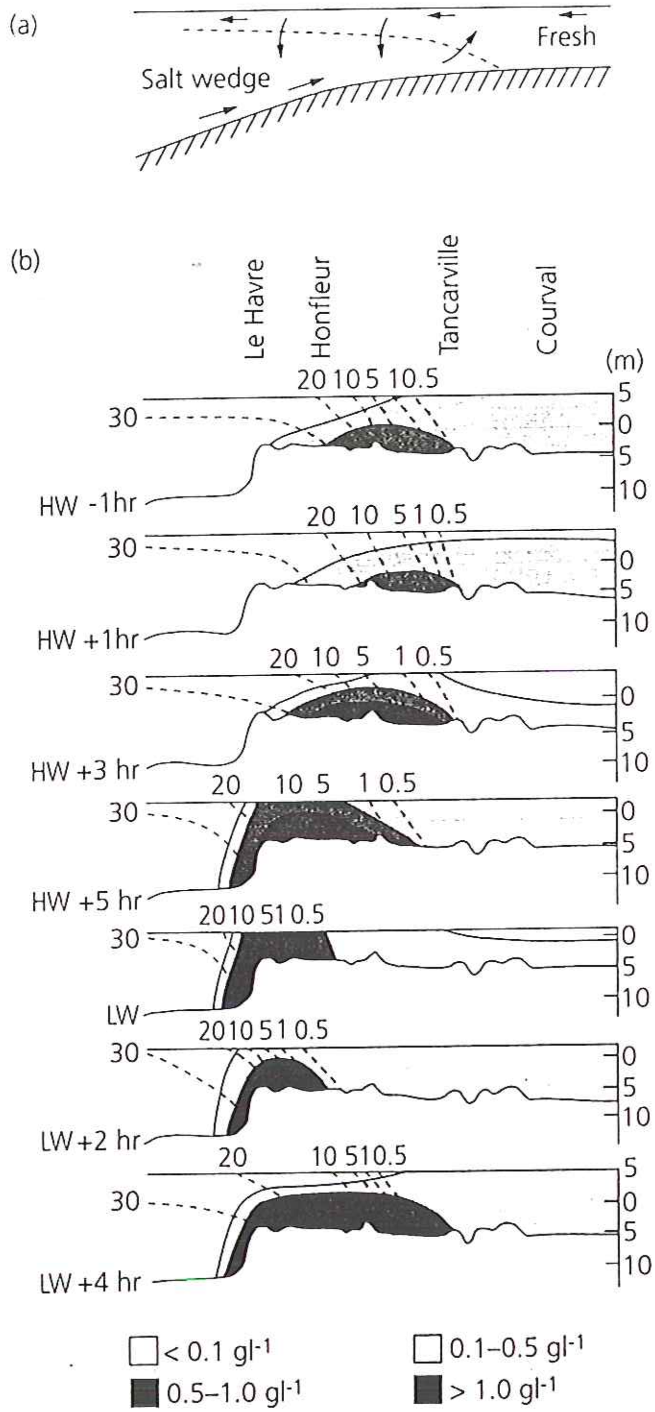

Fig. 7.17 (a) Schematic diagram to show the formation of the turbidity maximum in a partially mixed estuary. (b) The turbidity maximum in the Seine estuary, France, at intervals through a tidal cycle (at springs). The river discharge is 780 $m^3\ s^{-1}$. HW, high water; LW, low water; salinities in parts per thousand. After Avoine (1981) [19].

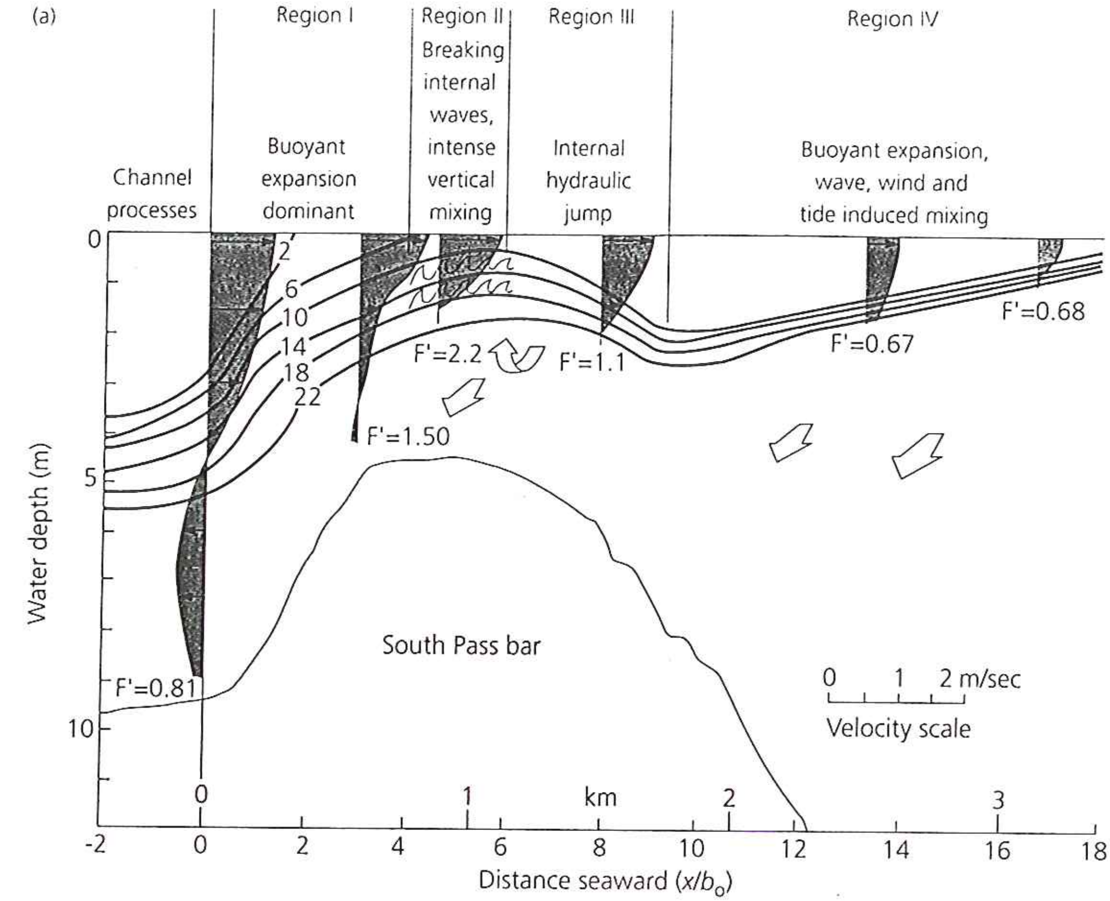

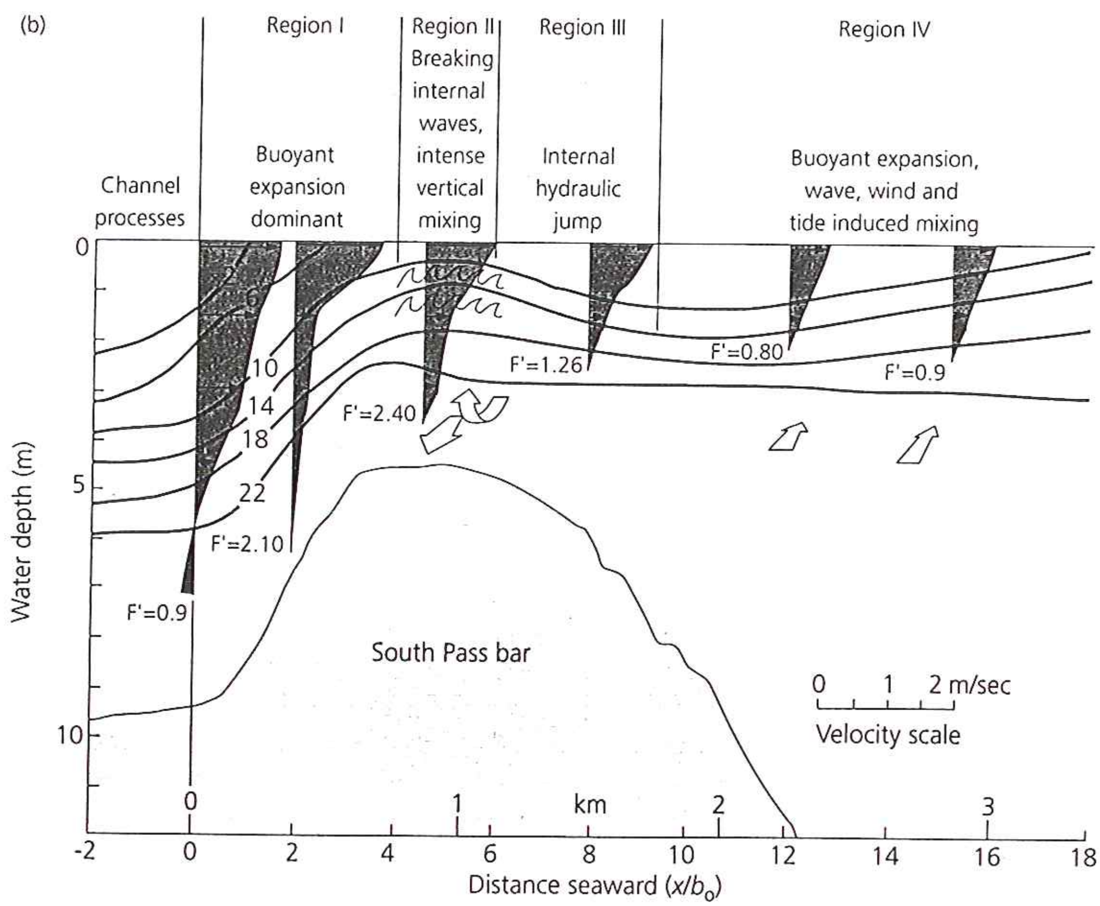

Fig. 7.10 Density (salinity) structure and flow pattern immediately seawards of the distributary mouth of South Pass during low discharge: (a) flooding tide; (b) ebbing tide. Hydrodynamic regions of Wright & Coleman (1974) [4] are shown. Note the intense vertical mixing due to internal waves and supercritical densimetric Froude numbers in region II. This causes deposition of sediment to form the South Pass bar.

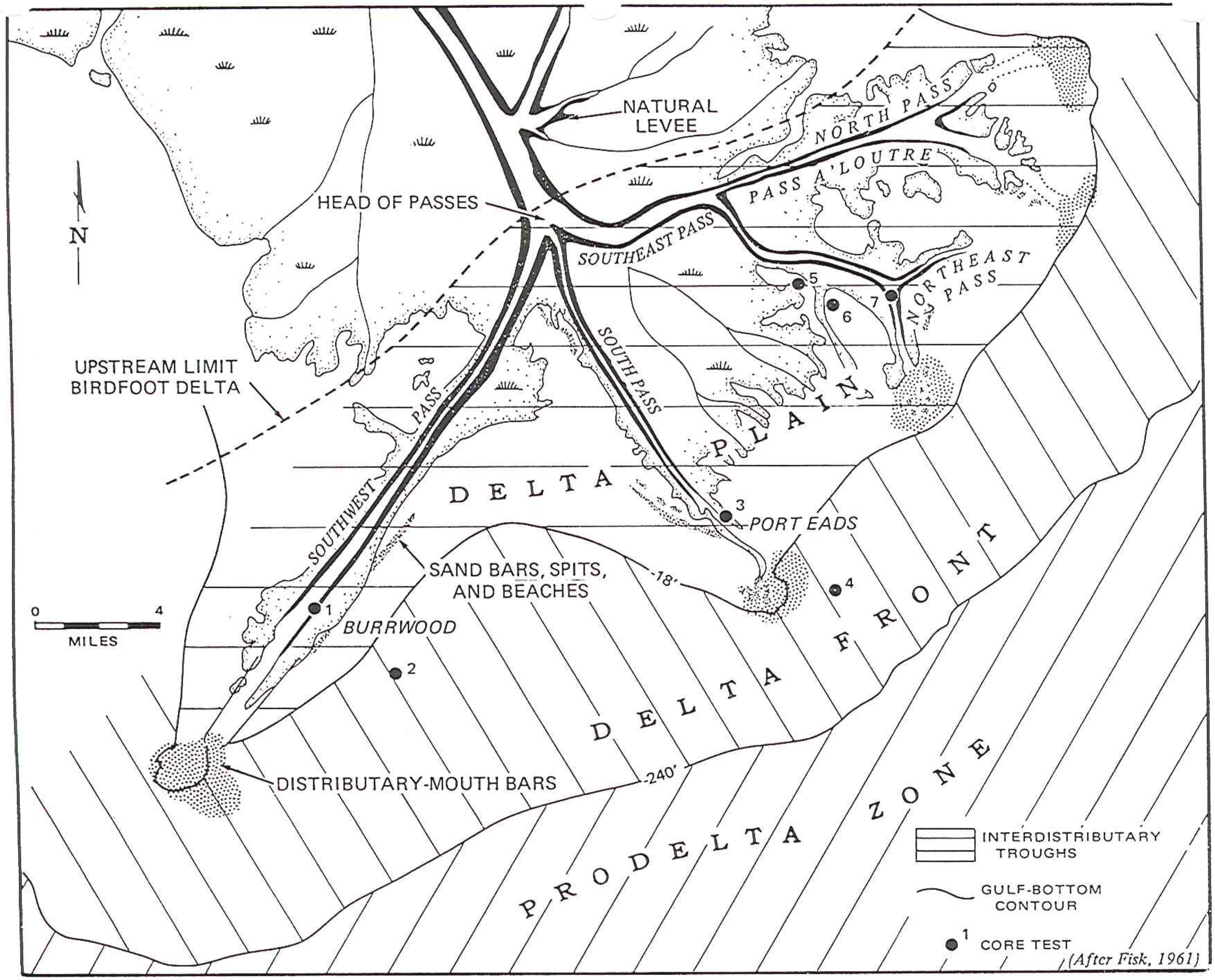

FIG. 17.—Depositional environments of Mississippi birdfoot delta.

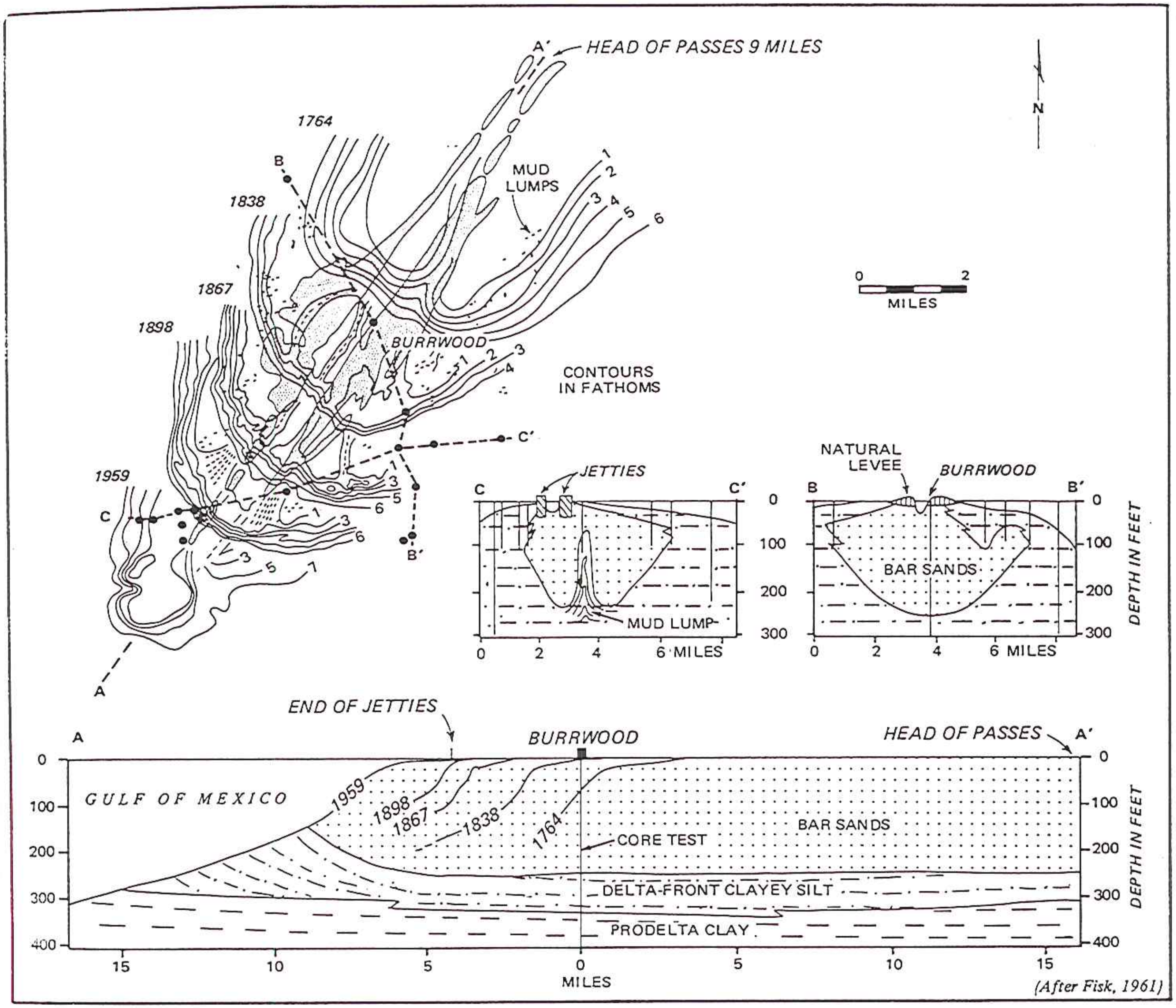

Fig. 20.—Historic development of Southwest Pass bar finger.

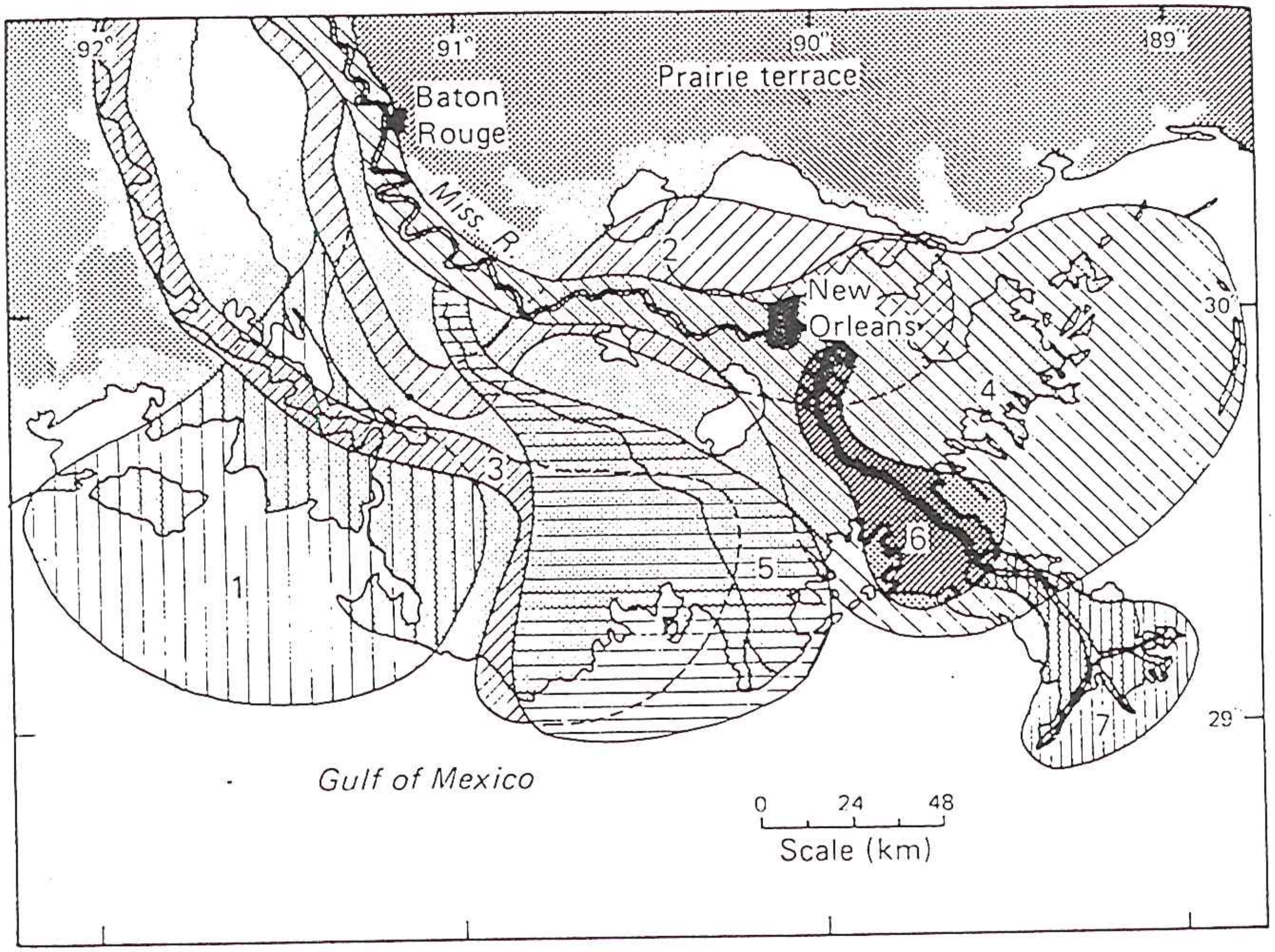

[pattern]	1	Sale Cypremort		>4600 yrs. B.P.
[pattern]	2	Cocodrie	*ca.*	4600-3500 yrs. B.P.
[pattern]	3	Teche	*ca.*	3500-2800 yrs. B.P.
[pattern]	4	St. Bernard	*ca.*	2800-1000 yrs B.P.
[pattern]	5	Lafourche	*ca.*	1000-300 yrs. B.P.
[pattern]	6	Plaquemine	*ca.*	750-500 yrs. B.P.
[pattern]	7	Balize		<550 yrs.

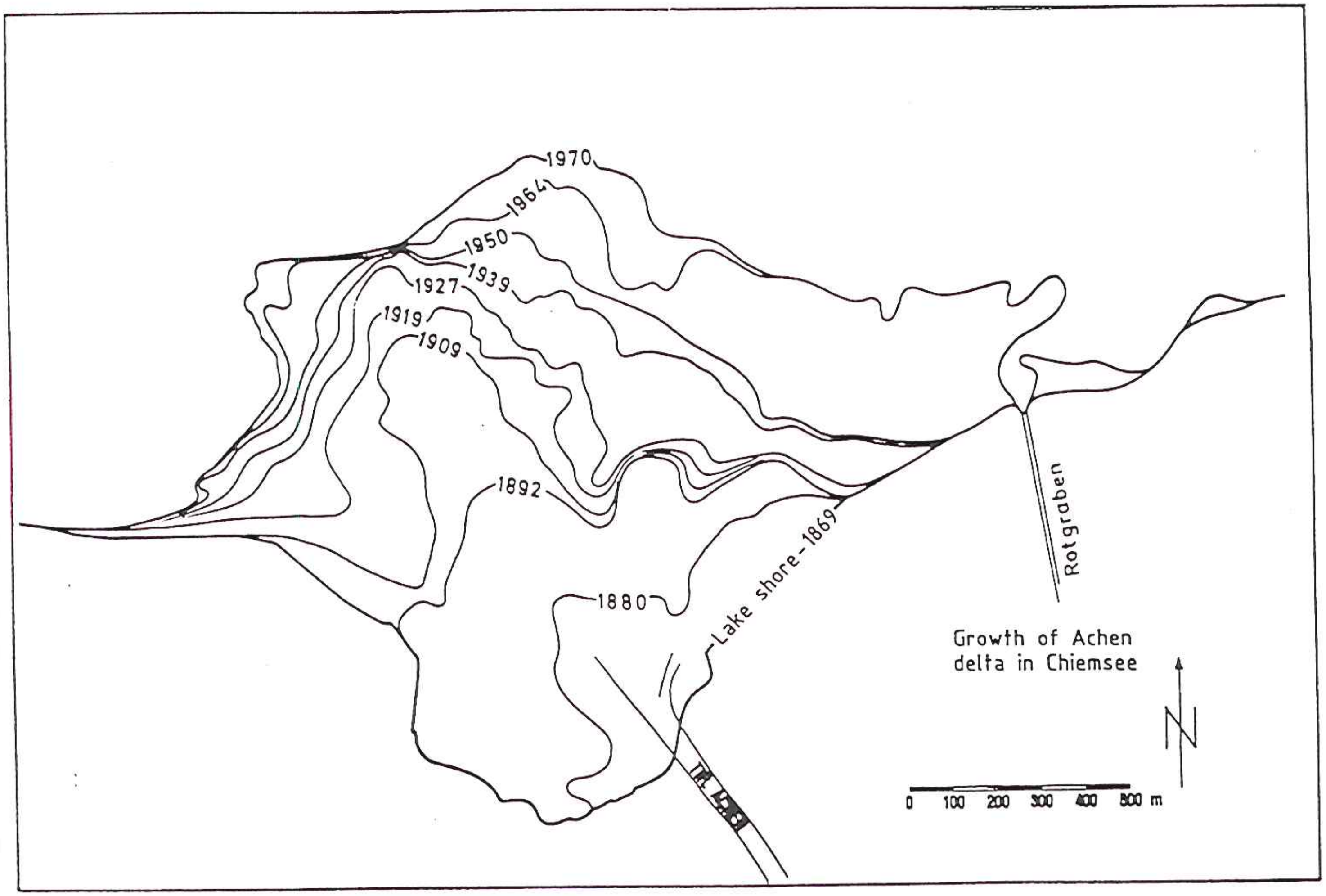

Fig. 4.7. Growth of delta of the Tyrolean Achen in the Chiemsee/Bavaria between 1869 and 1970

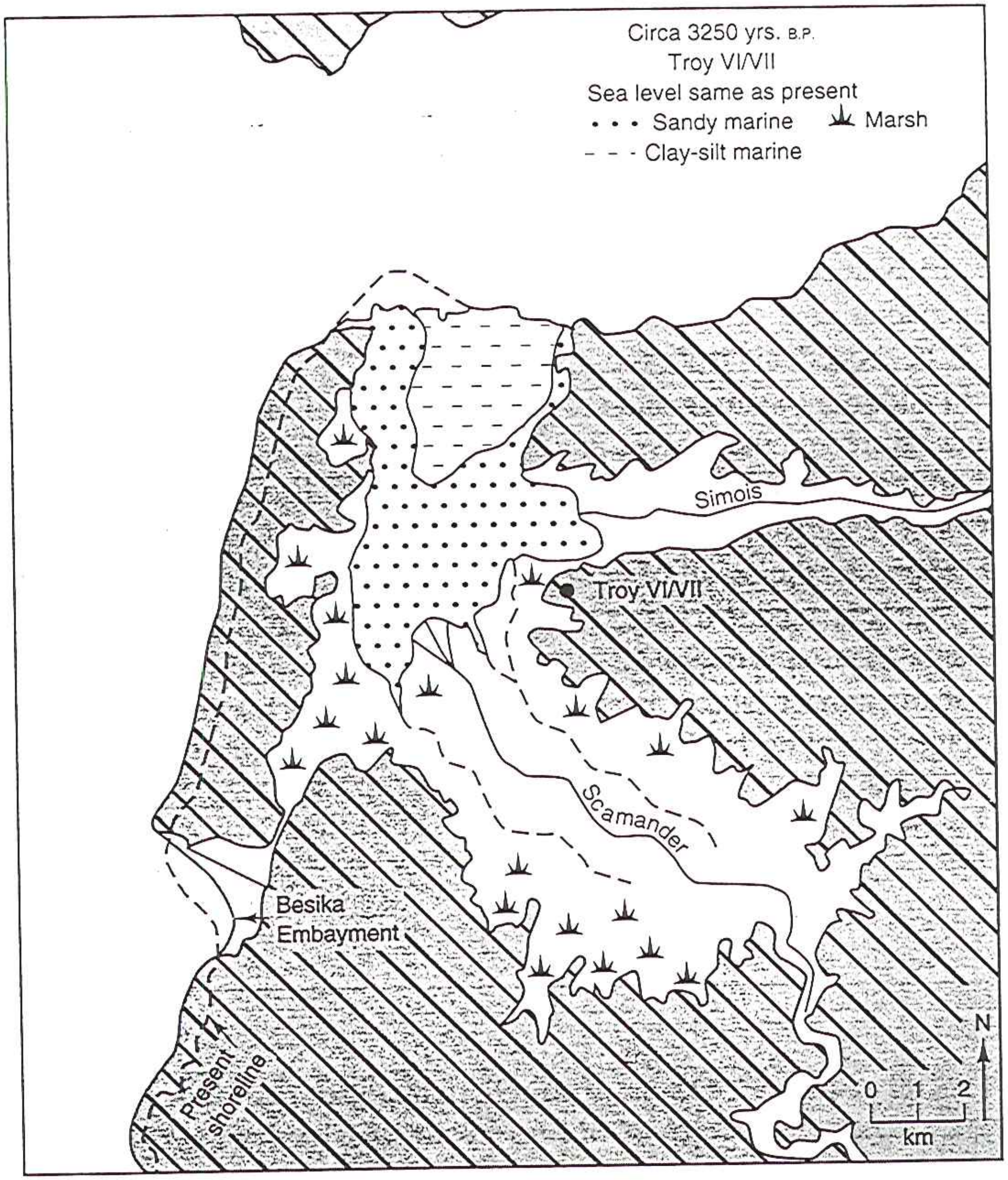

FIGURE 6–7 Radiocarbon-dated sediment cores from the plains around the ancient city of Troy show that it was a marine embayment at the time of the Iliad (3250 B.P.). (Courtesy of J. C. Kraft, University of Delaware.)

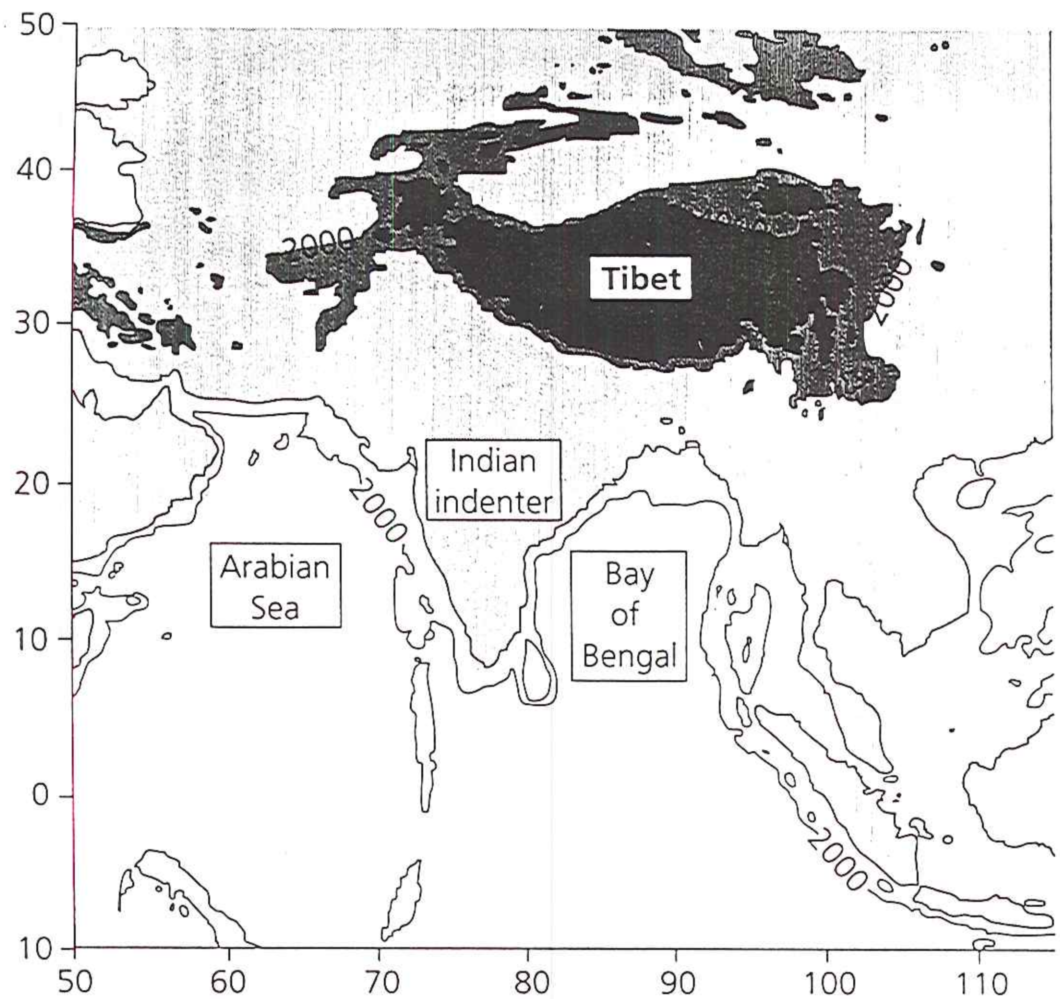

Fig. 1.28 Location of the collision zone of the Indian indenter with Asia and the resulting topography. Bathymetric contour at –2 km and topographic contours at 2 km and 4 km are shown. After Molnar *et al.* (1993) [31].

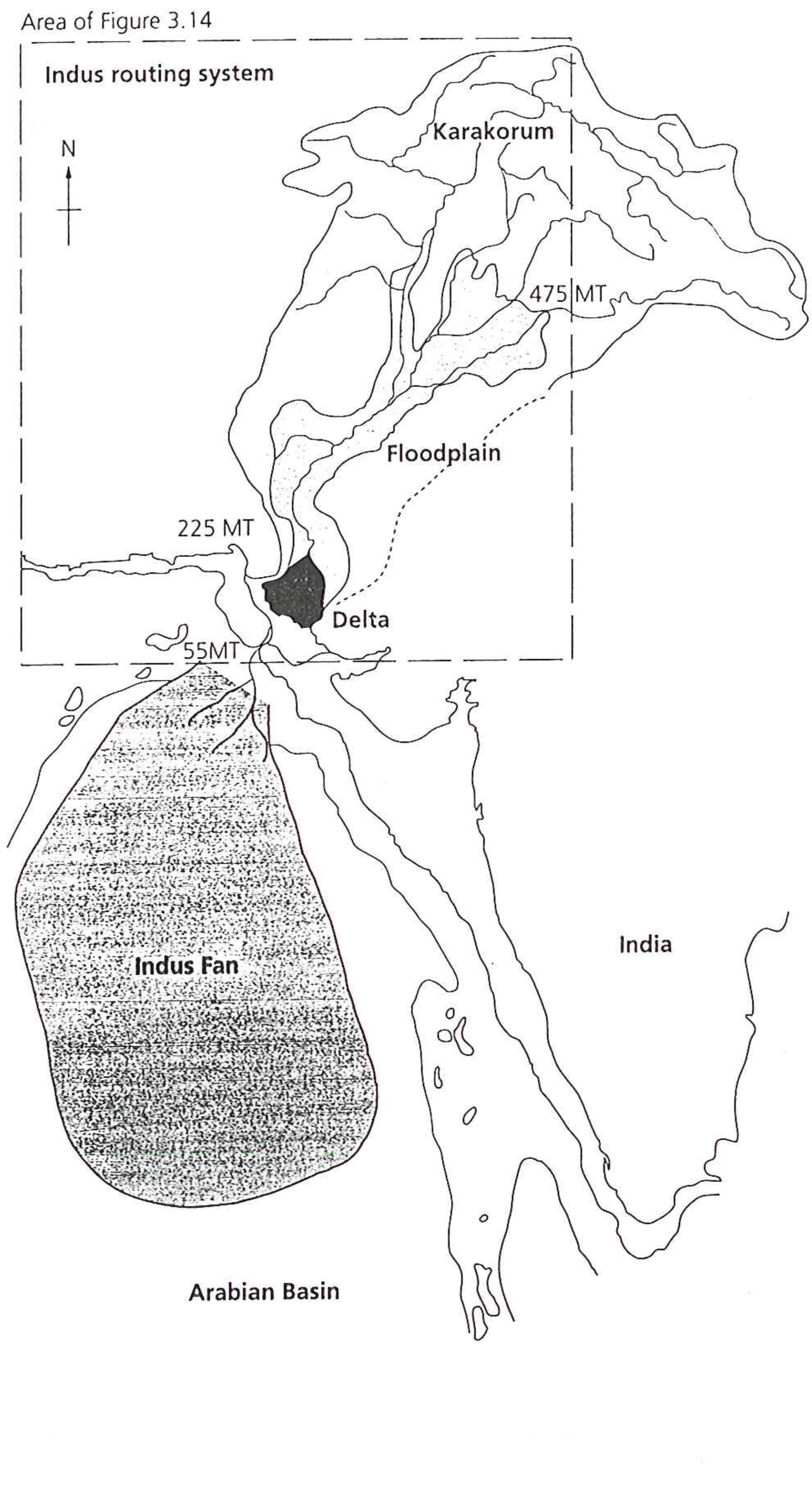

Fig. 3.13 The Indus sediment routing system, with sediment fluxes in megatonnes per year. After Milliman *et al.* (1994) [17].

TABLE 5.1 Major Rivers that Flow to the Sea, Listed in Order of Discharge

River	Location	Annual Discharge				
		Water (km^3/yr)	Dissolved Solids (Tg/yr)	Suspended Solids (Tg/yr)	Dissolved/ Suspended Ratio	Drainage Area (10^6 km^2)
1. Amazon	S. America	6300	275	1200	0.23	6.15
2. Zaire (Congo)	Africa	1250	41	43	0.95	3.82
3. Orinoco	S. America	1100	32	150	0.21	0.99
4. Yangtze (Chiang)	Asia (China)	900	247	478	0.53	1.94
5. Brahmaputra	Asia	603	61	540	0.11	0.58
6. Mississippi	N. America	580	125	210 (400)	0.60	3.27
7. Yenisei	Asia (Russia)	560	68	13	5.2	2.58
8. Lena	Asia (Russia)	525	49	18	2.7	2.49
9. Mekong	Asia (Vietnam)	470	57	160	0.36	0.79
10. Ganges	Asia	450	75	520	0.14	0.975
11. St. Lawrence	N. America	447	45	4	11.3	1.03
12. Parana	S. America	429	16	79	0.20	2.6
13. Irrawaddy	Asia (Burma)	428	92	265	0.35	0.43
15. Mackenzie	N. America	306	64	42	1.5	1.81
17. Columbia	N. America	251	35	10 (15)	3.5	0.67
20. Indus ← #20	Asia (India)	238	79	59 (250)	1.3	0.975
Red (Hungho)	Asia (Vietnam)	123	?	130	?	0.12
Huanghe (Yellow)	Asia (China)	59	22	1100	0.02	0.77

Note: Tributaries are excluded. Tg = 10^6 tons = 10^{12} g.

Sources: Water and suspended solids from Milliman and Meade (1983) and Milliman and Syvitski (1992). Dissolved solids calculated from Table 5.7 and Pinet and Souriau (1988) (for the Irrawaddy). Suspended load values in parentheses indicate pre-dam values.

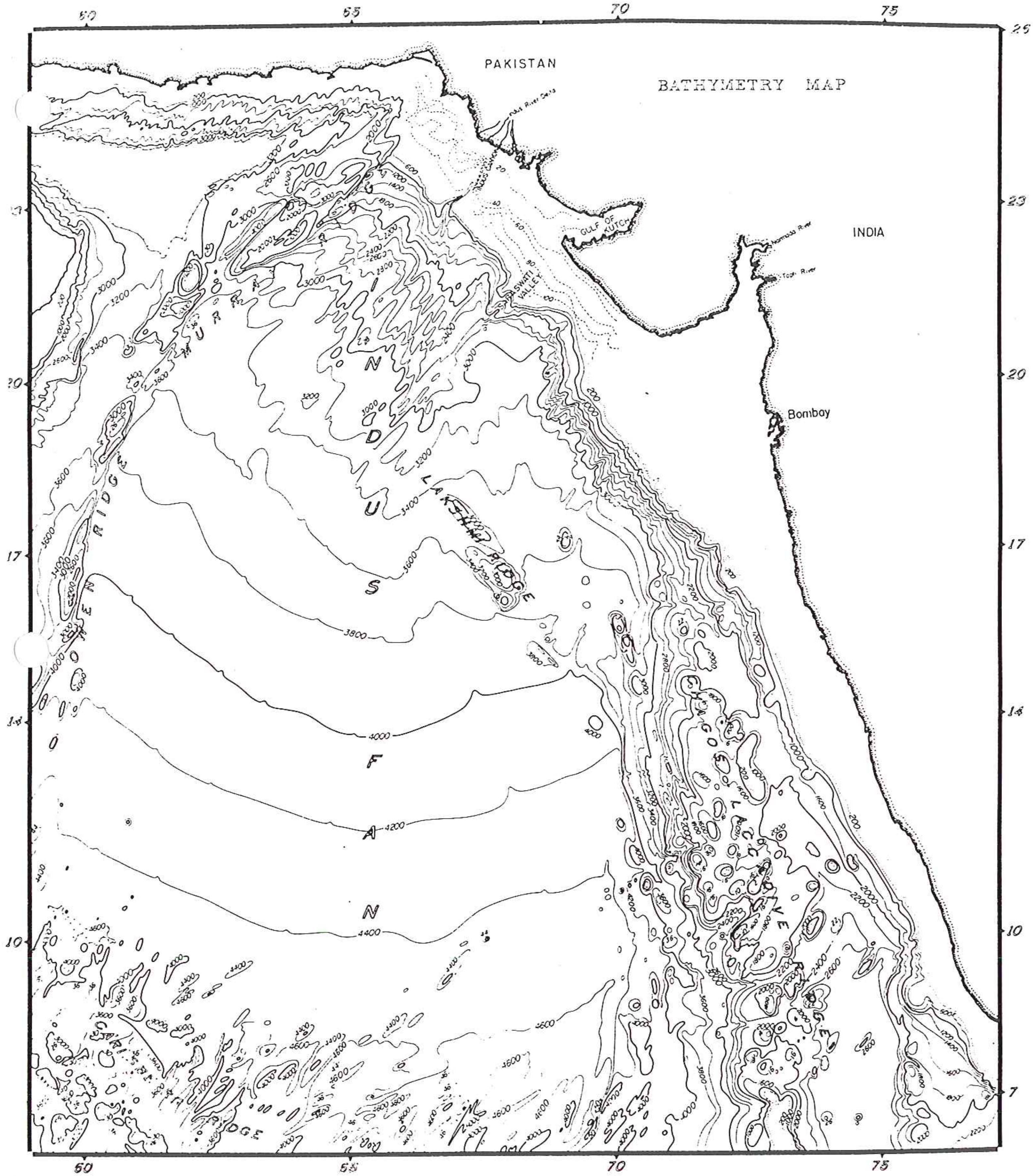

Fig. 2. Bathymetry of the Arabian Sea contours in meters compiled by U.S. Naval Oceanographic Office. Note the irregular topography n the upper Indus Fan resulting from channel-levee build-ups.

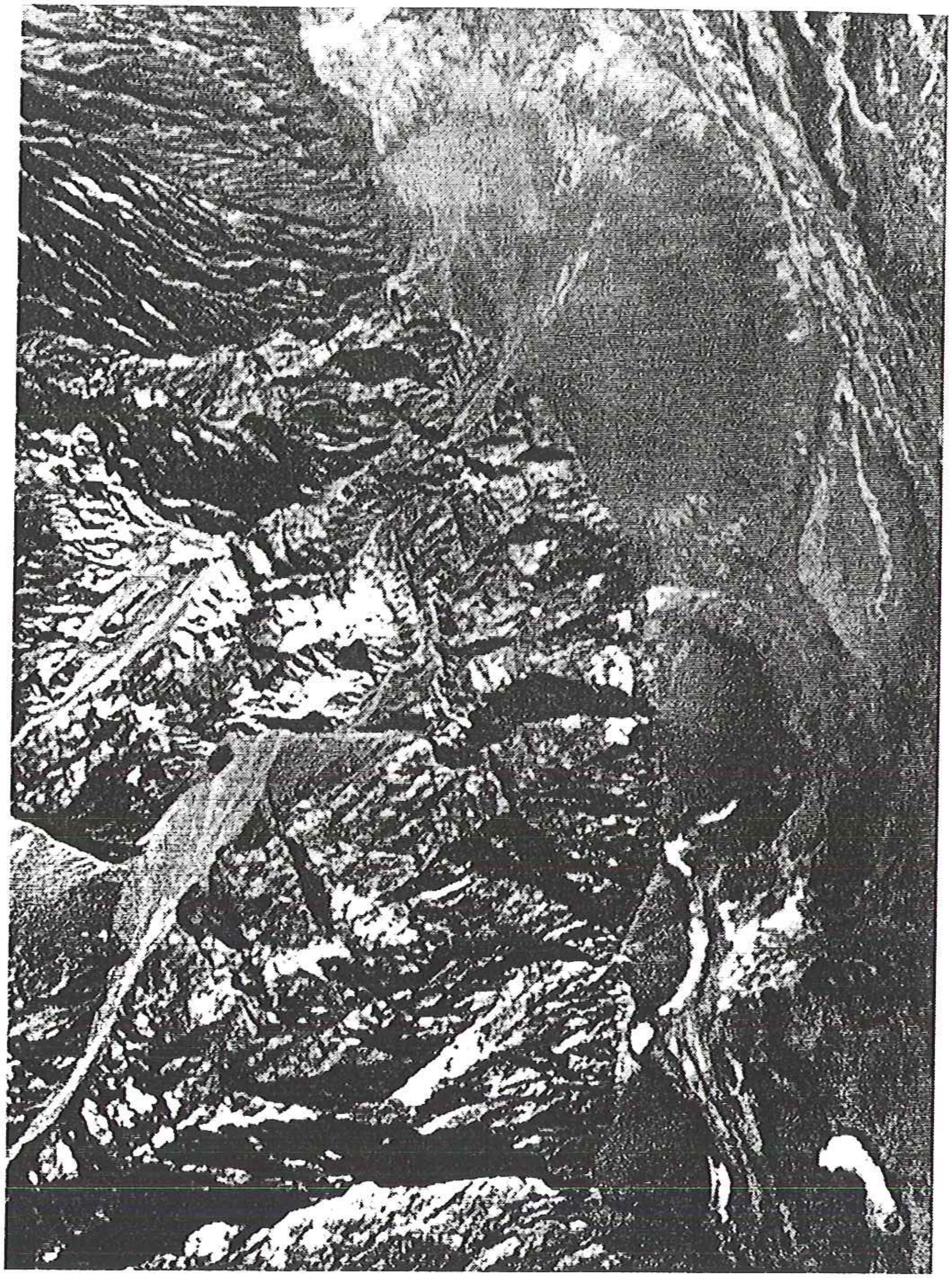

FIGURE 14.38 Alluvial fans in Death Valley, California. The varying sizes of fans relate to the varying sizes of the drainage basins providing material to the fans. The larger the drainage basin, the larger the fan. The biggest fan shown here has a radius of about 2.5 km. *(Fairchild Aerial Photograph Collection, Whittier College)*

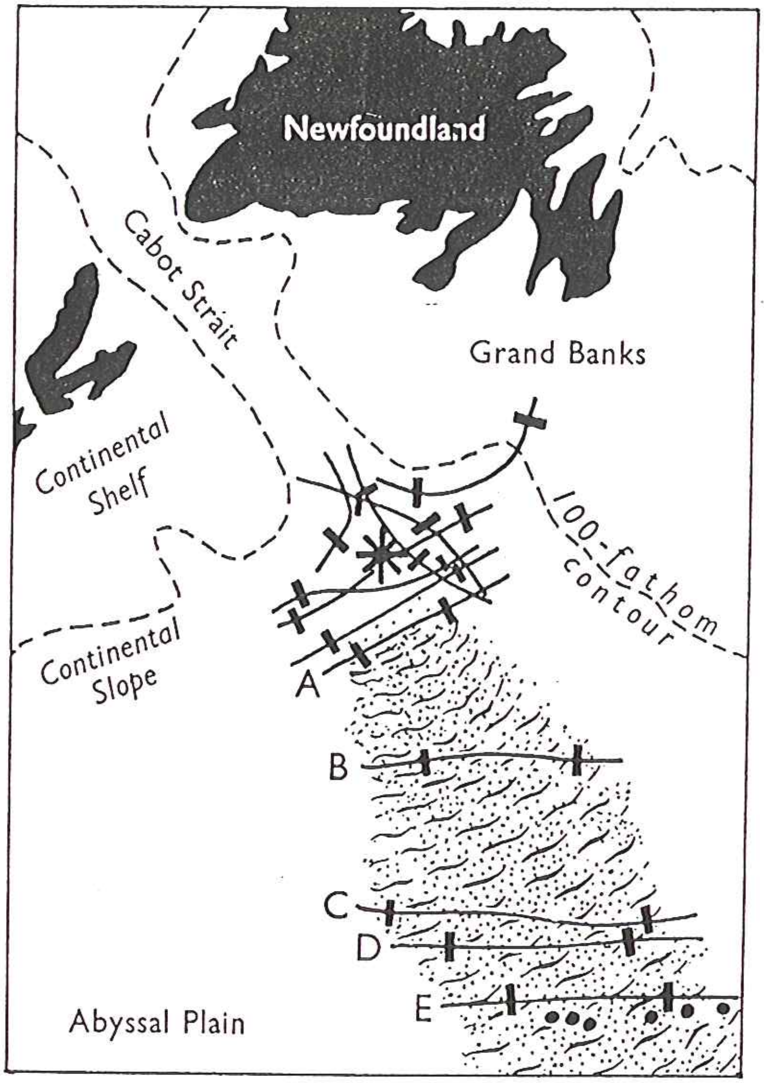

FIG. 654 Sketch map showing the original positions of the 12 broken telegraph cables crossing the deep continuation of the Cabot Strait submarine canyon at the time of the Grand Banks earthquake of 1929. Breakages are shown by cross bars. The shaded area represents the submarine canyon within which the cables marked A to E were broken and twisted and the loose parts carried away and/or buried in sediment. The large star at the head of this area marks the epicentral region of the earthquake, i.e. the region immediately above its place of origin (see p. 903). The black circles south of cable E are the sites from which cores were brought up. (*After J. W. Gregory, Nature*, 1929; *and B. C. Heezen and M. Ewing*, 1952)

FIG. 655 Profile of floor of Cabot Strait submarine canyon, with arrows showing the places where the cables marked A to E were broken and the corresponding time intervals after the earthquake, which originated at 20:32 G.M.T. on 18 November 1929. Length of section approximately 610 miles (*After B. C. Heezen and M. Ewing*, 1952)

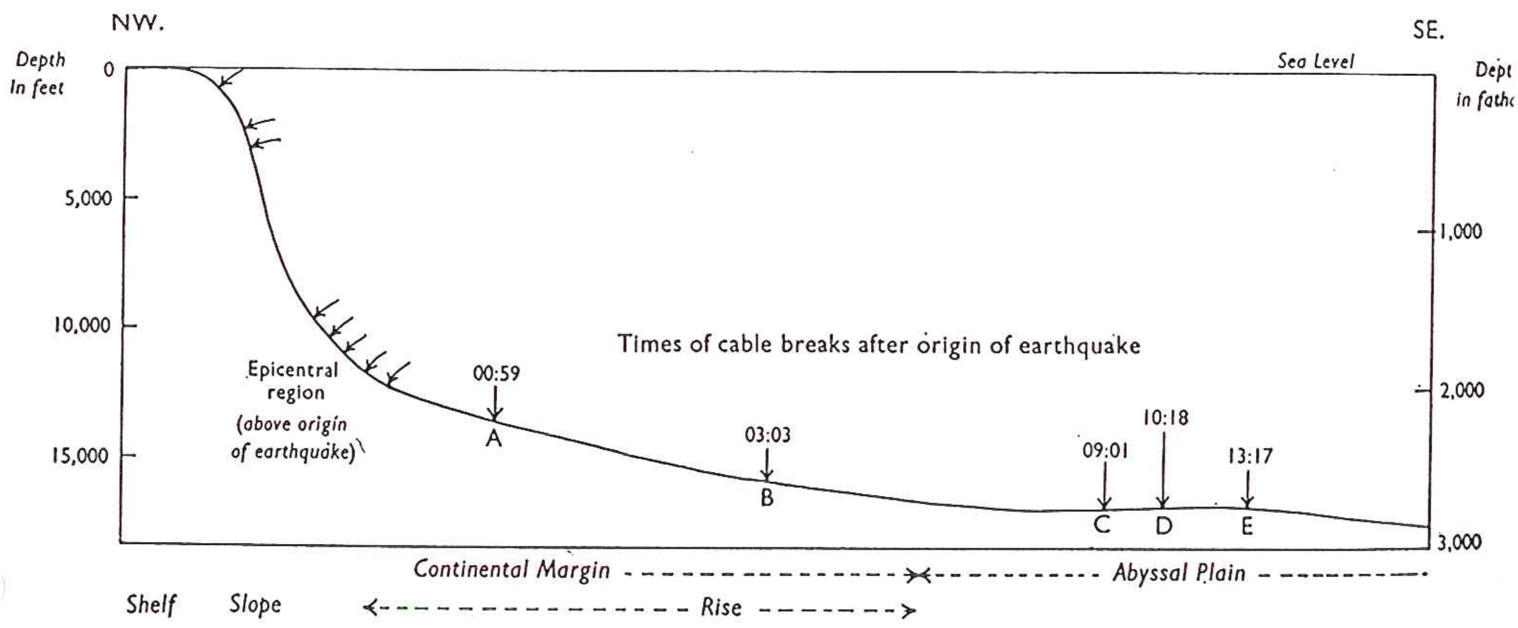

Grand Banks earthquake of 1929 —
triggered a turbidity flow
(submarine landslide)

Broke 12 trans-Atlantic telephone cables
(before satellite transmission)

Flow came down Cabot Strait — a
deep submarine valley cut into
continental shelf

From time intervals could deduce
speed

50 mph at point A, slowing
down until finally fades out

Heezen & Ewing predicted that
this single slide should cover
250,000 km² of Atlantic seafloor
average thickness 40 – 100 cm.
0.4 – 1 meter in thickness

Confirmed by deep-sea coring

Turbidite deposits very characteristic — graded
bedding 

in alternating layers —
each a single landslide

Figure 5.21 from Judson & Richardson

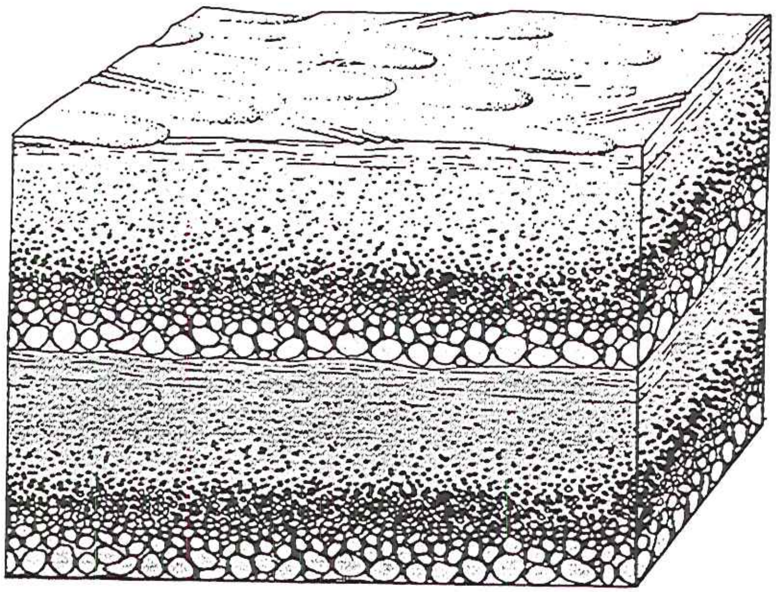

Figure 5.6 **Graded bedding** is produced by turbidity currents. It occurs in widespread layers, each layer generally less than a meter thick. Deep-marine environments commonly produce a great thickness of graded layers, which can easily be distinguished from sediment deposited in most other environments.

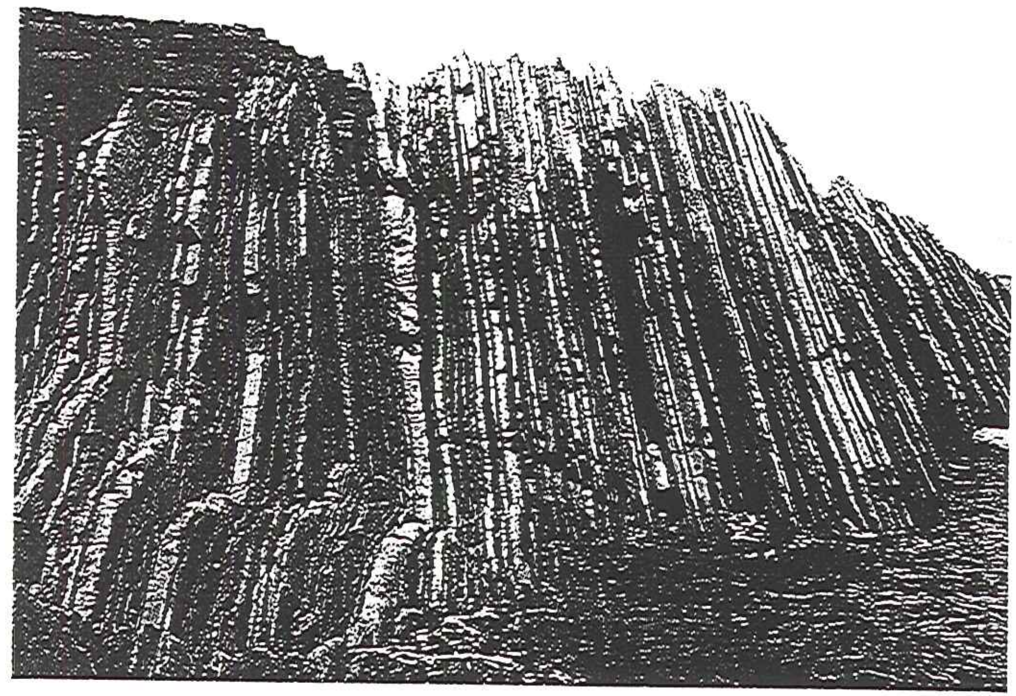

FIGURE 5.21 Turbidites near Zumaya in northern Spain have been tilted on end. The rhythmic nature of the bedding is characteristic of turbidites. *(Franklyn B. Van Houten)*

Illustrate with a somewhat simpler example — the <u>Indus Fan</u> — before returning to example of Mississippi.

40 Myr ago, India collided with Eurasia, formed the Himalaya Mountains & Tibetan Plateau (Fig 1.28)

Rugged relief & monsoon climate ⟹ erosion rates of Himalaya extremely high.

Headwaters > 4 km elevation

<u>Indus River</u> in Pakistan drains Karakoram region of high Himalaya. Figure 3.13 shows the Indus delta, the tributaries in the high Himalaya and the submarine <u>Indus Fan</u> in the Arabian Sea

Note that the fan area ≃ area of the catchment basin ≈ 10^6 km²

The sediment discharge rates from the <u>high mountains</u> are

~~600 ... ≈ 6~~

figure says $475 \cdot 10^6$ tons/yr

$$500 \cdot 10^6 \text{ tons/yr} = 5 \cdot 10^{11} \text{ kg/yr}$$

More than half of this is redeposited in the low plains (floodplain) above the delta.

Prior to ~1950 the discharge at the delta was ~ <u>250 · 10^6 tons/yr</u>

Economic development led to the building of a number of hydroelectric & irrigation dams which are now trapping most of this sediment

< 50 · 10^6 tons/yr now

Major impact of man in last 50 years — Indus is #20 river in terms of discharge

Let us do a simple <u>sediment budget</u> calculation for the Indus.

Assume rate 250 · 10^6 tons/yr for entire 40 Myr.

Total amount of sediment delivered

<u>10^{16} tons = 10^{19} kg</u>

We wish to compare this with the volume of the sediments in the Indus cone.

The relevant density is that of the compacted sediments — compaction due to weight of overlying sediments (Xiao & Suppe data)

$$\rho = 2700 \text{ kg/m}^3$$

$$\frac{10^{19} \text{ kg}}{2700 \text{ kg/m}^3} = 3.7 \cdot 10^{15} \text{ m}^3$$

> $V_{Indus} = 3.7 \cdot 10^{6} \text{ km}^3$
>
> ↑ volume of compacted eroded sediments

Let us compare this with the volume of the Indus cone.

Model as a portion of a cone of height h and radius a

$$V = \frac{1}{8} \cdot \underbrace{\frac{1}{3}\pi h a^2}$$

↖ 45° cone — volume of complete cone

a doorstop

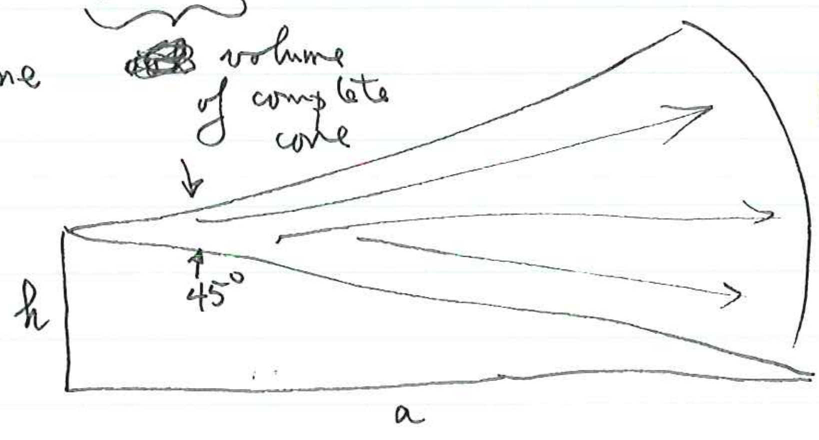

$V_{\text{Indus cone}} = 3.7 \cdot 10^6 \text{ km}^3$

$h = \frac{24}{\pi a^2} (3.7 \cdot 10^6)$

a (from map) = 1500 km

$\boxed{h = 12 \text{ km}}$

Fig. 8 shows the sediment thickness measured by seismic reflection

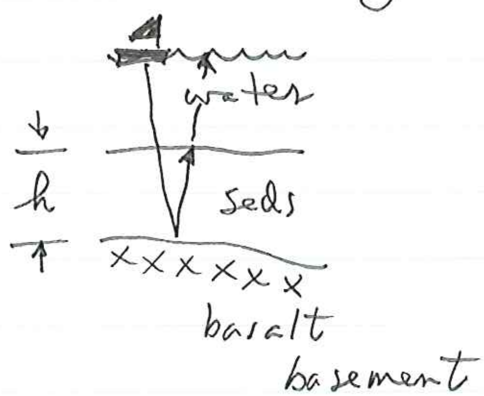

$\text{two-way time} = \frac{2h}{v}$

$h = \frac{vt}{2}$

$v_{\text{seds}} \approx 4 \text{ km/s} \Rightarrow$

$h \text{ (km)} \approx 2 \times \text{time (secs)}$

Maximum delay times near delta are ~ 6 sec ~ <u>12 km</u>

So, we see that the sediment budget balances.

We can do a similar calculation for the Mississippi River.

The major sediment source for the Mississippi is the Cordilleran mtn belt — i.e., the Continental Divide.

These mountains were constructed during the Laramide orogeny ~ 100 Myr ago

The Mississippi & its tributaries have also been affected by damming & other flood control measures.

Currently ~ $200 \cdot 10^6$ tons/yr suspended sediment load (Table 5.1) — but the pre-colonization value thought to be twice this — $400 \cdot 10^6$ tons/yr.

This is 1.6 × Indus ⇒

$$V_{Miss} = (1.6)(3.7 \cdot 10^6 \text{ km}^3)\left(\frac{100 \text{ Myr}}{40 \text{ Myr}}\right)$$

$$\boxed{V_{Miss} = 1.5 \cdot 10^7 \text{ km}^3}$$

In this case the basin is better modelled as a half-cylinder

radius a

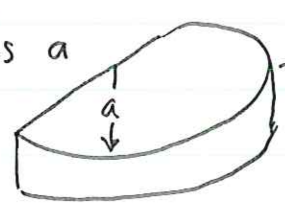

} depth h

~~a ≈ 800 km~~

a ≈ 1000 km

$$V_{basin} = \frac{1}{2} \pi a^2 h$$

half cone

$$h = \frac{V_{seds}}{\frac{1}{2}\pi a^2} = \frac{1.5 \cdot 10^{7} \text{ km}^3}{\frac{\pi}{2} (1000 \text{ km})^2}$$

$h \simeq 10$ km average depth

Actual depth varies between 5 – 15 km

See Figs. 20, 11–18 and 12 — all based on interpretation of seismic reflection data.

Note also the presence of the salt domes — highly vertically exaggerated in all the figures.

Gulf of Mexico was an evaporite basin in the Cretaceous, prior to the Laramide — sediments deposited on a thick layer of salt.

Salt very mobile — plastic substance — flows upward in Diapirs — oil is trapped above these, as discussed in Part IV of this course.

Isostasy

Say full of sediments

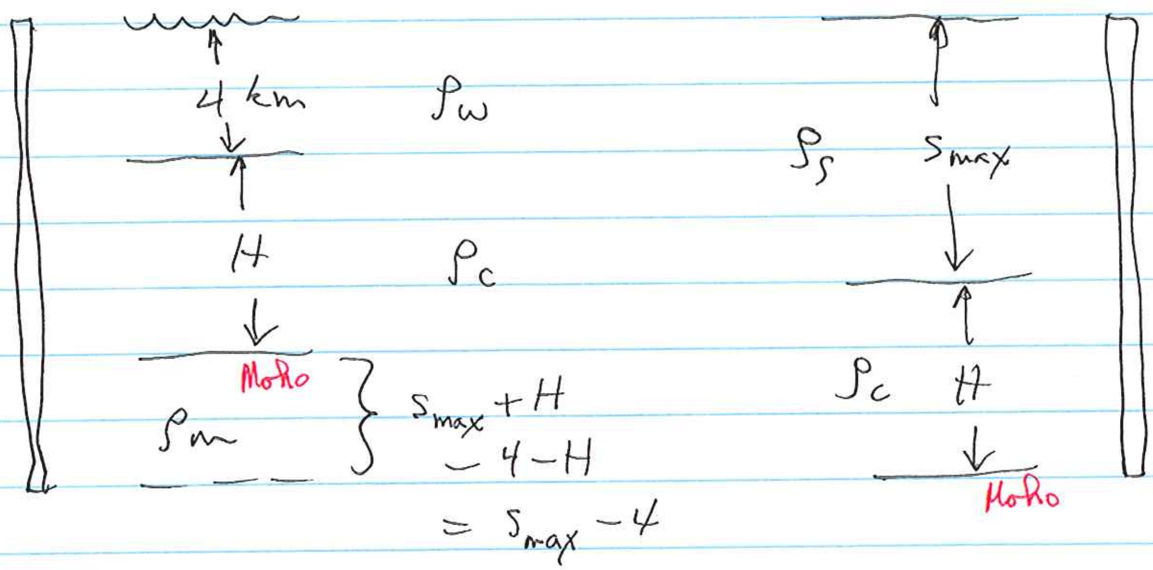

$$\rho_w \cdot 4 + \rho_c H + \rho_m (s_{max} - 4)$$

$$= \rho_s s_{max} + \rho_c H$$

crustal thickness cancels out

independent of H & ρ_c

$$s_{max} = \left(\frac{\rho_m - \rho_w}{\rho_m - \rho_s} \right) 4$$

$$= \left(\frac{3300 - 1000}{3300 - 2700} \right) \times 4$$

$$= \underline{15 \text{ km}}$$

The sediment accumulations in both the Indus & Mississippi cones — and along all passive continental margins, e.g., the Atlantic margin of the US — are 10 – 15 km thick

The average depth of the oceans is only 4 km. How is it possible to deposit 10 – 15 km of sediments in only 4 km of water?

Answer — isostasy — the underlying crust sinks beneath the accumulating sediments.

How thick a layer of sediments can be deposited in an ocean basin of initial depth D — problem from Exam Prep Sheet #2.

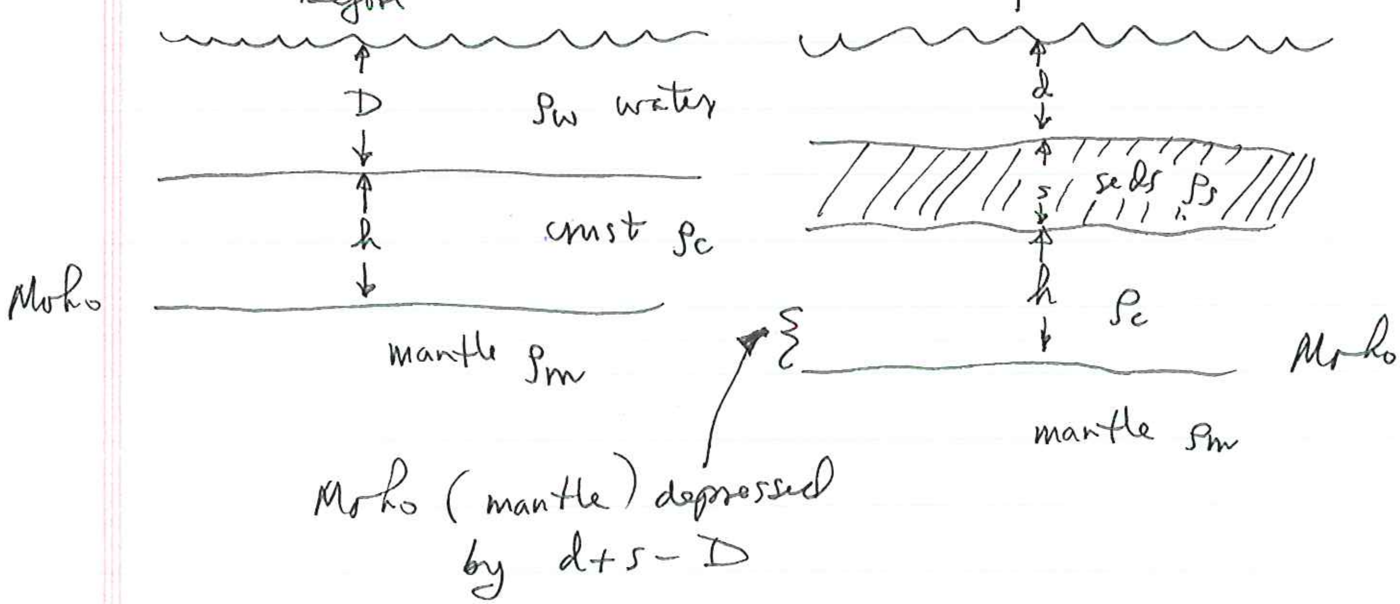

Equating equal columns:

$$\rho_w D + \rho_c h + \rho_m (d + s - D) = \rho_w d + \rho_s s + \rho_c h$$

cancel — crustal thickness doesn't matter

$$(\rho_m - \rho_s) s = (\rho_m - \rho_w)(D - d)$$

$$\boxed{s = \left(\frac{\rho_m - \rho_w}{\rho_m - \rho_s}\right)(D - d)}$$

$\rho_m = 3300 \text{ kg/m}^3$
$\rho_w = 1000 \text{ kg/m}^3$
$\rho_s = 2700 \text{ kg/m}^3$ (compacted)

A 4 km deep ocean basin is full to the brim if $d = 0$.

$$s_{max} = \left(\frac{3300 - 1000}{3300 - 2700}\right) \times 4 \text{ km}$$

$$\boxed{s_{max} = 15 \text{ km}}$$ — in good agreement with observations

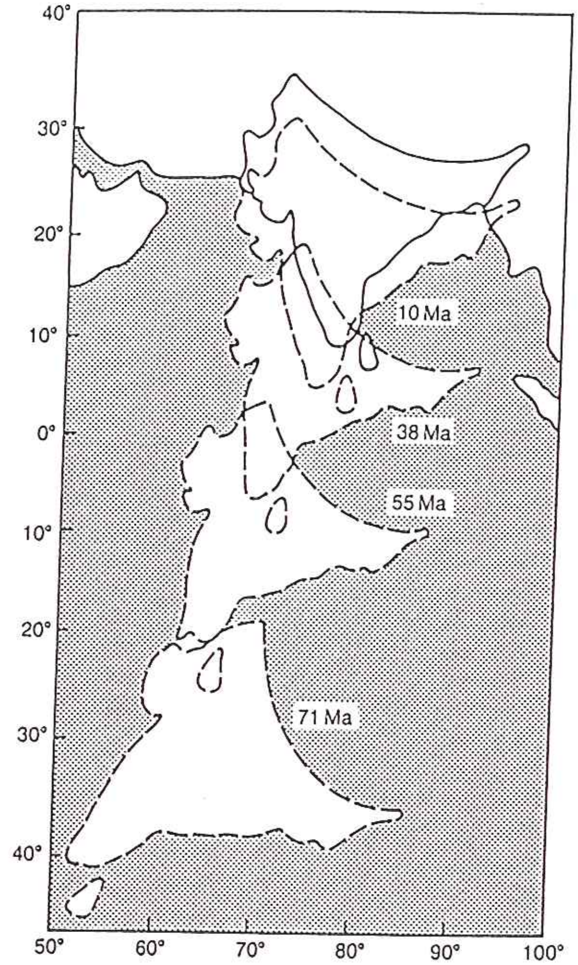

Fig. 9.12 Northward drift of India with respect to Asia for the period 71 Ma to present determined from magnetic lineations in the Indian and Atlantic Oceans (redrawn from Molnar & Tapponnier, 1975, *Science*, 189, 419–26, with permission from the AAAS. Copyright © 1975 by the AAAS).

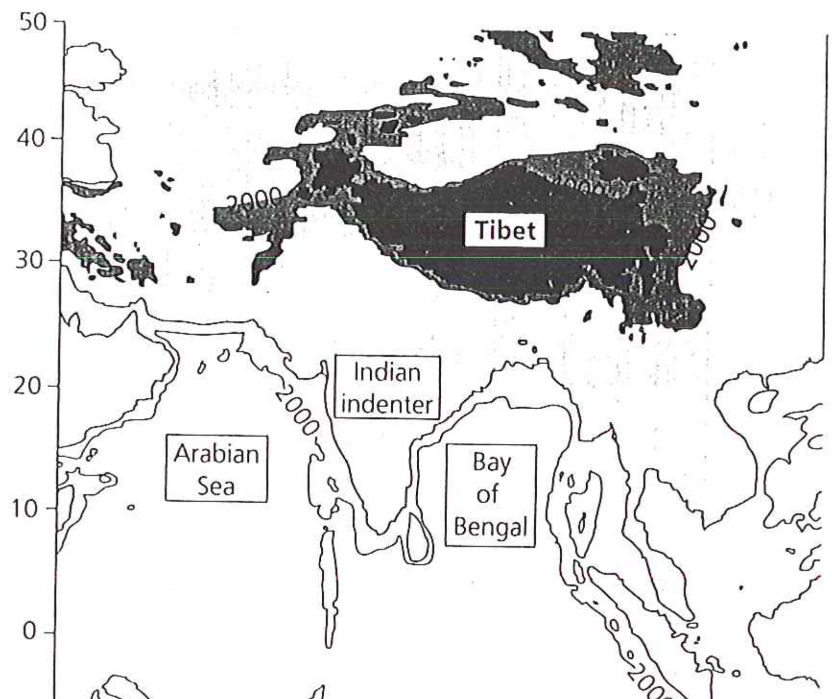

Fig. 1.28 Location of the collision zone of the Indian indenter with Asia and the resulting topography. Bathymetric contour at −2 km and topographic contours at 2 km and 4 km are shown. After Molnar *et al.* (1993) [31].

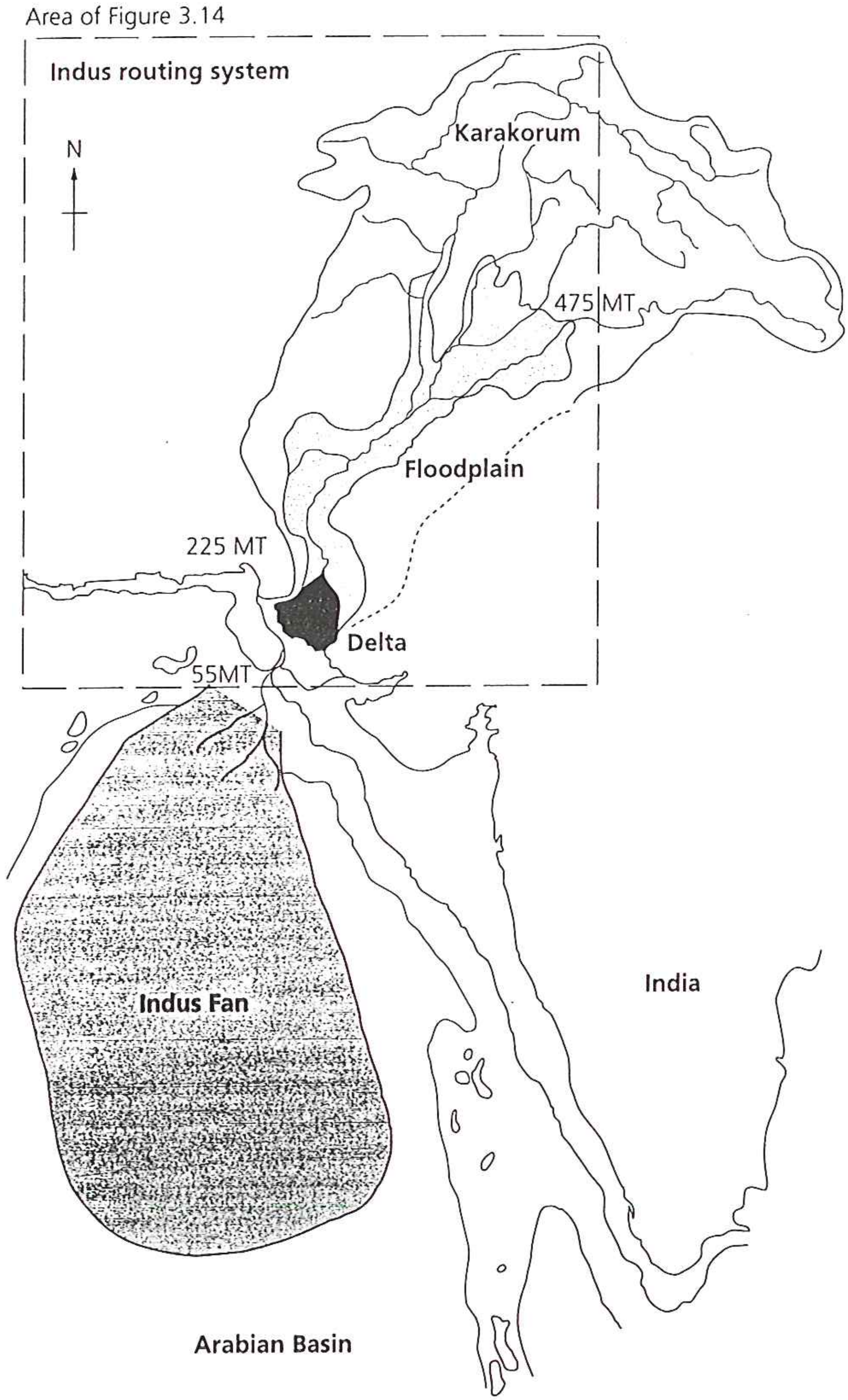

Fig. 3.13 The Indus sediment routing system, with sediment fluxes in megatonnes per year. After Milliman *et al*. (1994) [17].

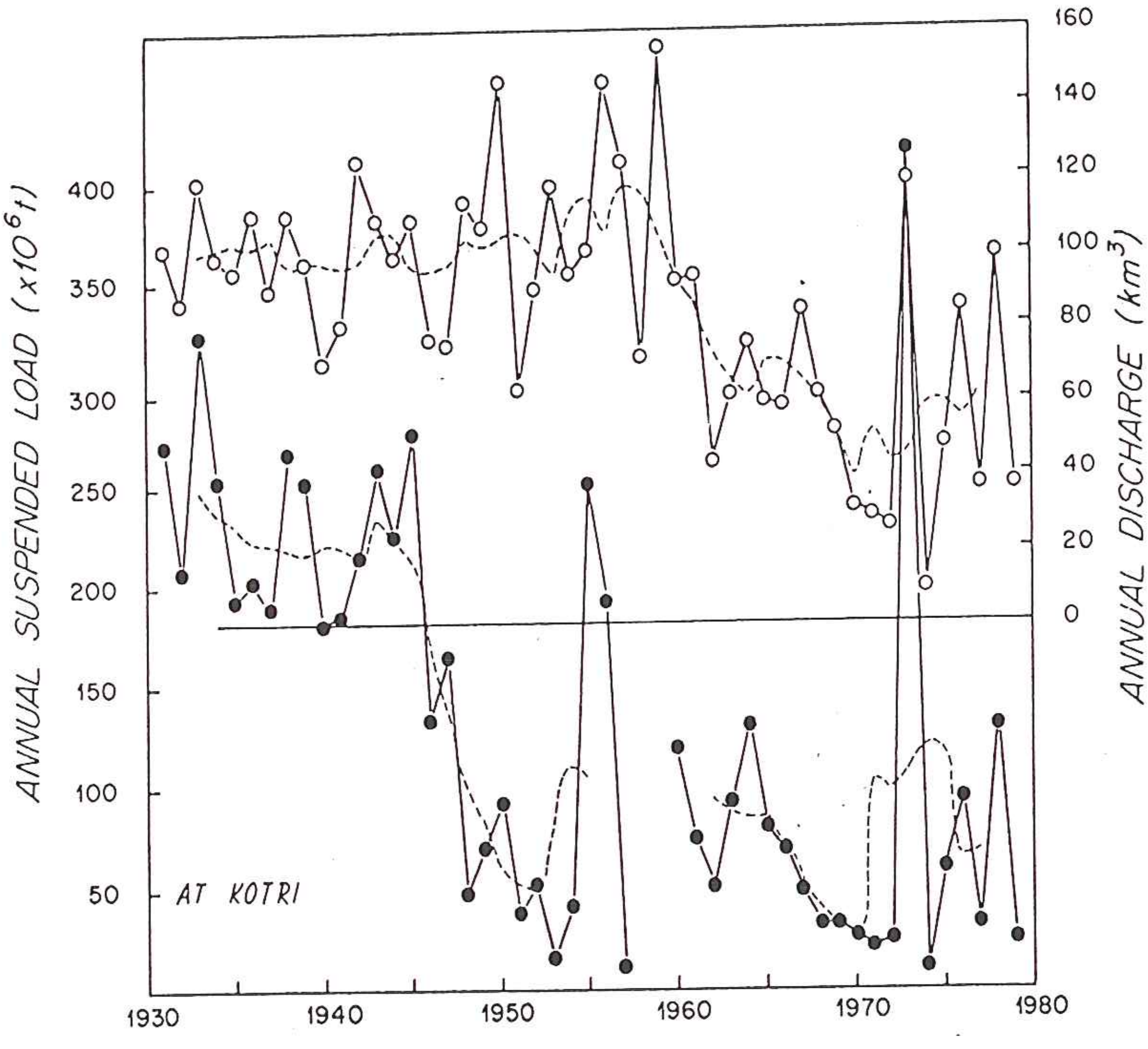

Figure 8. Discharge and sediment loads for the Indus River at Kotri, 1931-1979. Dashed lines represent 5-yr running mean averages. Data from the Indus River Commission.

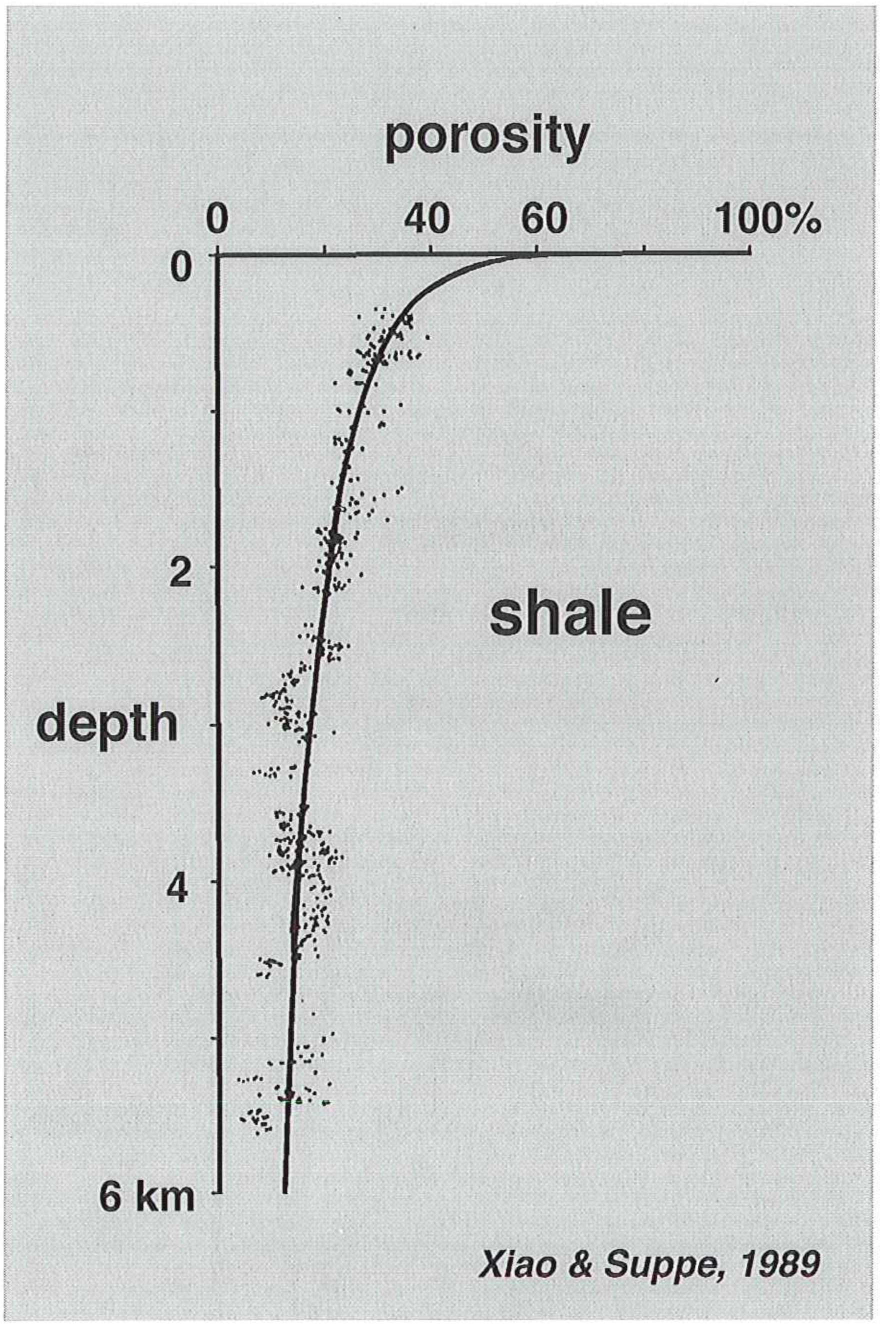
porosity
0
40
60
100%
0
2
4
6 km
depth
shale
Xiao & Suppe, 1989

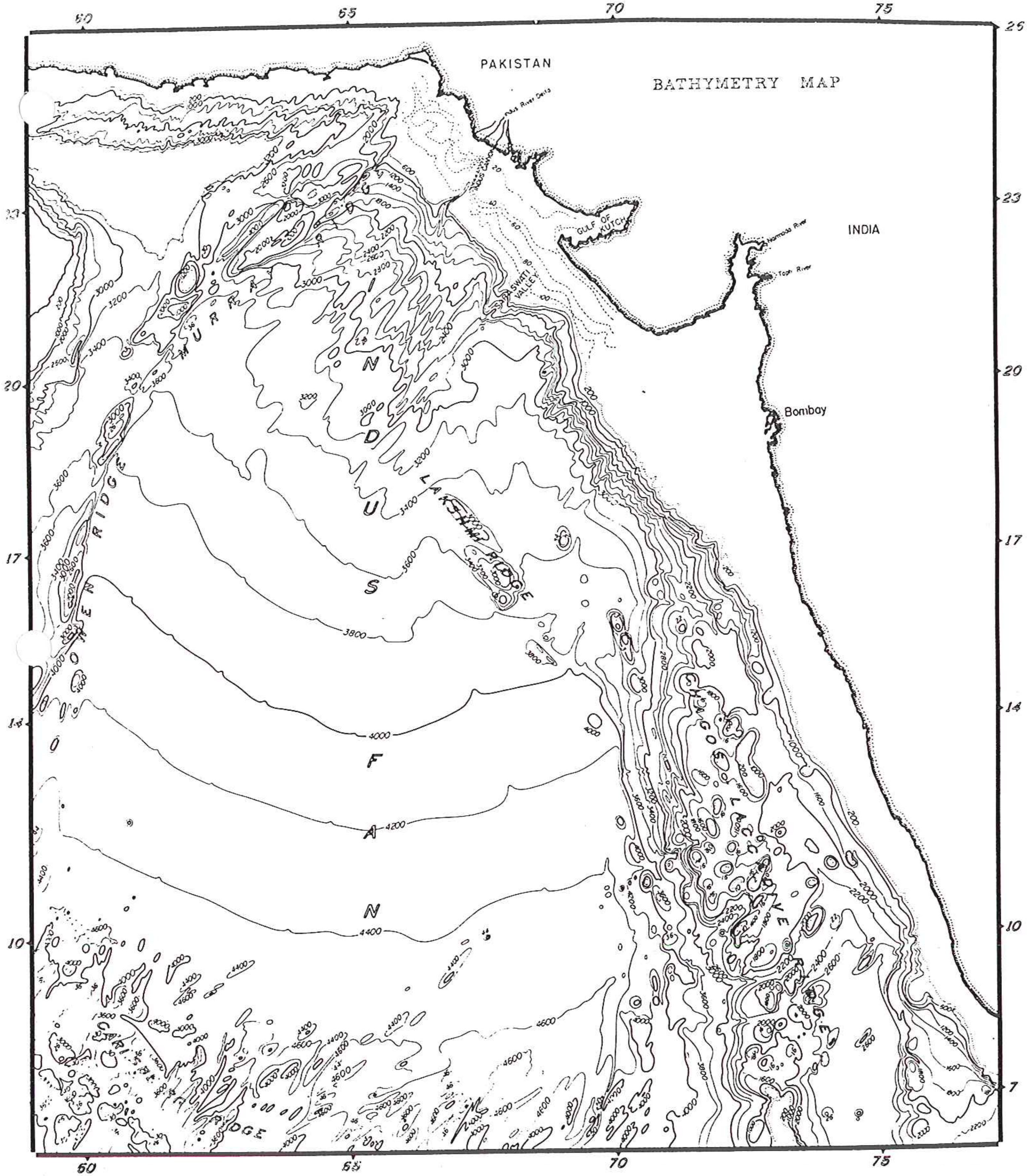

Fig. 2. Bathymetry of the Arabian Sea contours in meters compiled by U.S. Naval Oceanographic Office. Note the irregular topography n the upper Indus Fan resulting from channel-levee build-ups.

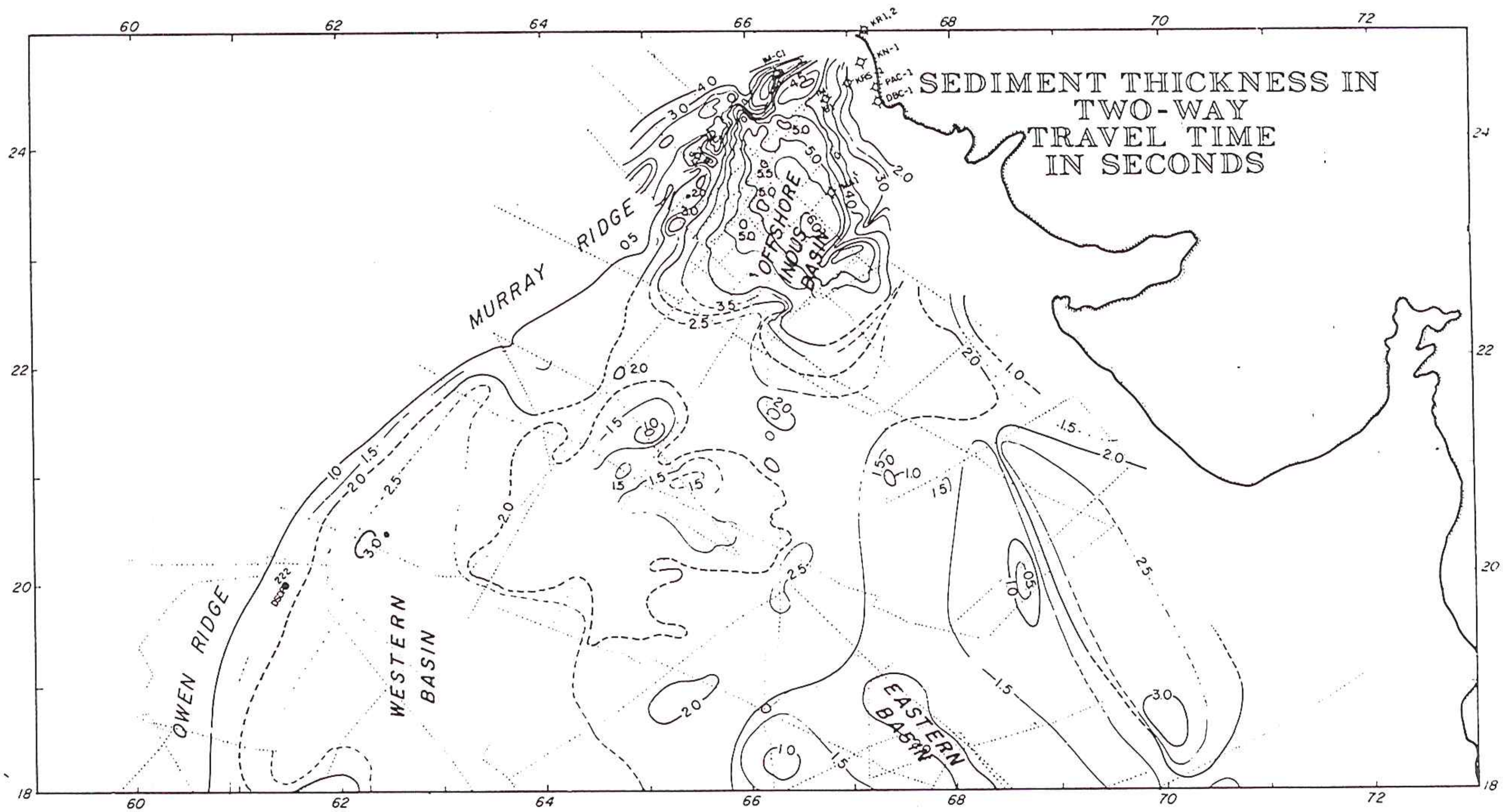

Fig. 8. Sediment-thickness distribution in seconds of two-way travel time. Note three major depocenters: Offshore Indus Basin, Western Basin and Eastern Basin.

1 second two-way travel time = 2 km depth

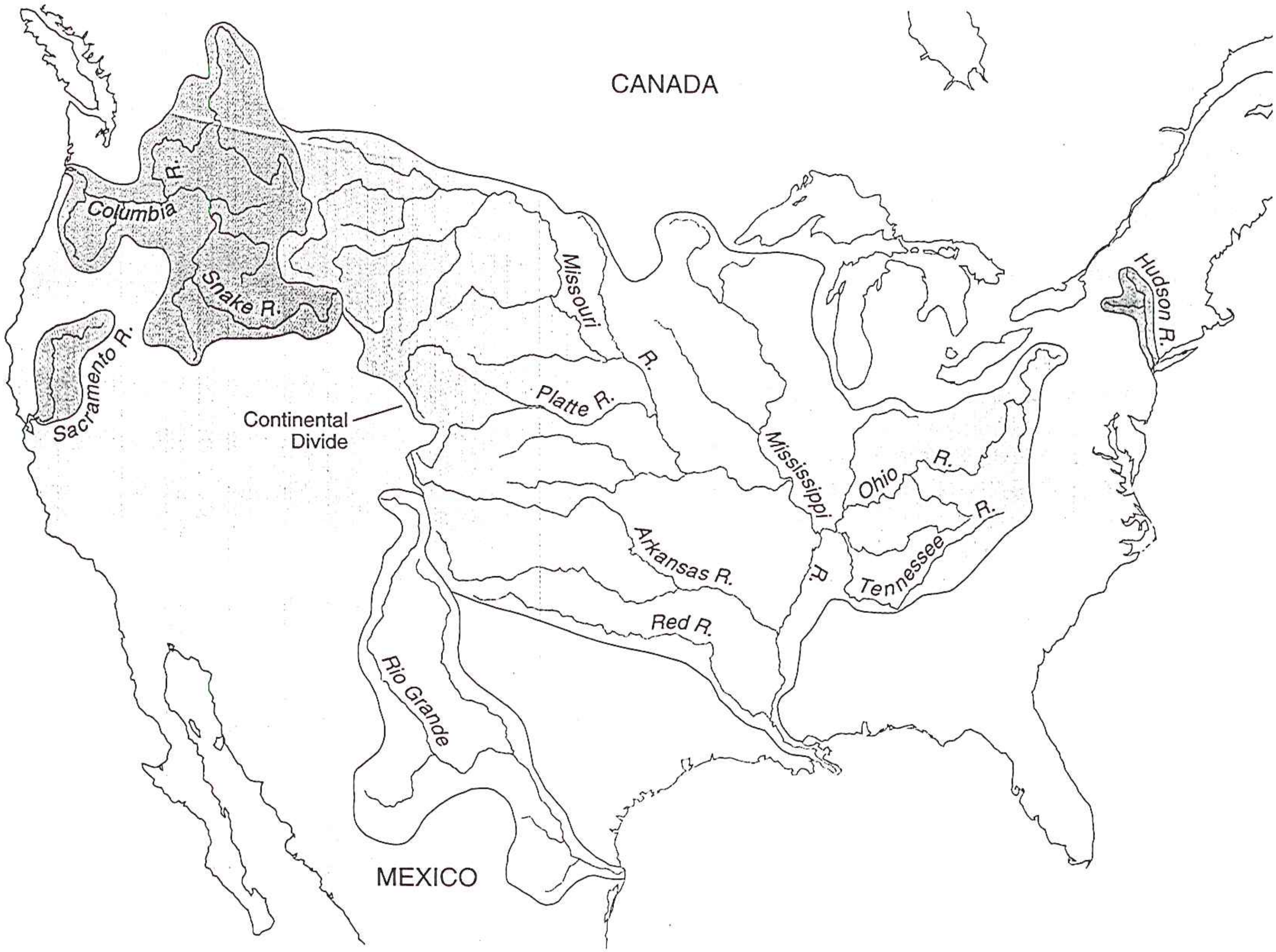

FIGURE 14.19 The stream's drainage basin is the area from which the stream and its tributaries receive water. Some well-known drainage basins in North America are shown here.

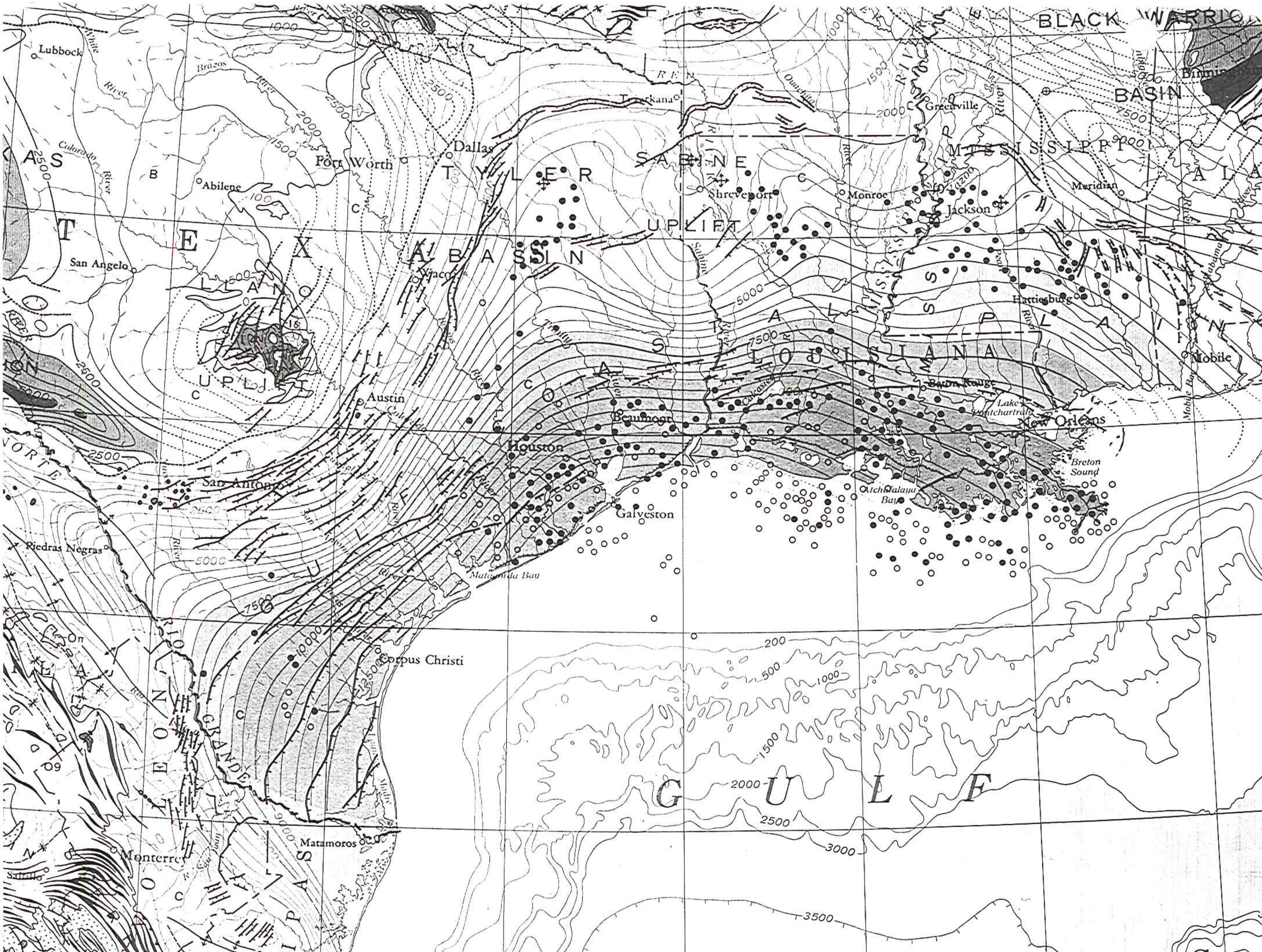

BLACK WARRIOR
BASIN
MISSISSIPPI
TYLER
SABINE
UPLIFT
BASIN
TEXAS
LLANO
UPLIFT
LOUISIANA
GULF
Lubbock
Abilene
Fort Worth
Dallas
Texarkana
Shreveport
Monroe
Greenville
Jackson
Meridian
Hattiesburg
Mobile
Baton Rouge
Lake Pontchartrain
New Orleans
Breton Sound
Atchafalaya Bay
Beaumont
Houston
Galveston
Matagorda Bay
Waco
Austin
San Antonio
San Angelo
Piedras Negras
Corpus Christi
Matamoros
Monterrey
RIO GRANDE
Brazos River
Colorado River
Sabine
Trinity
Red River
200
500
1000
1500
2000
2500
3000
3500
5000
7500
10,000

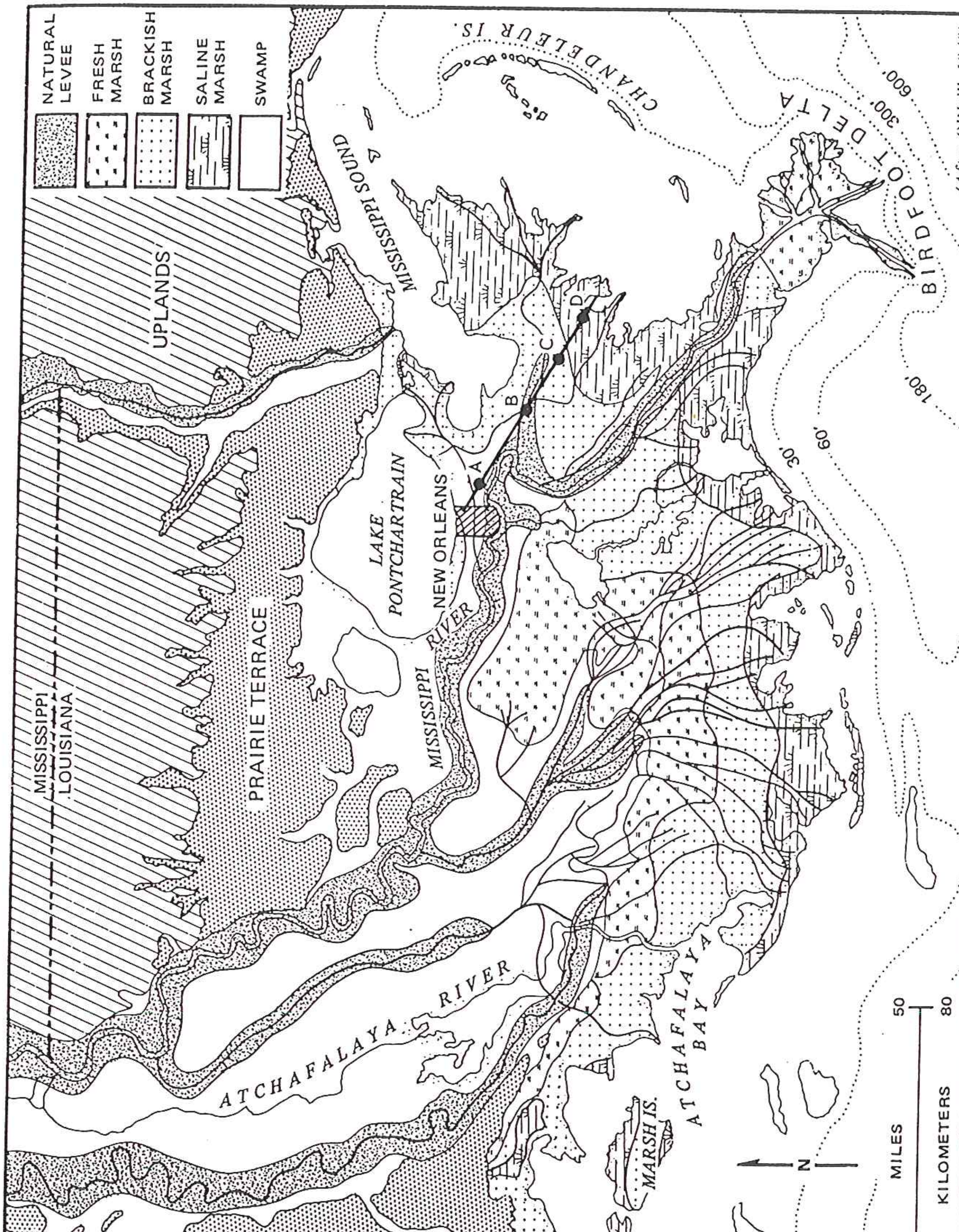

FIG. 8.—Distribution of swamp and marsh environments on Mississippi deltaic plain.

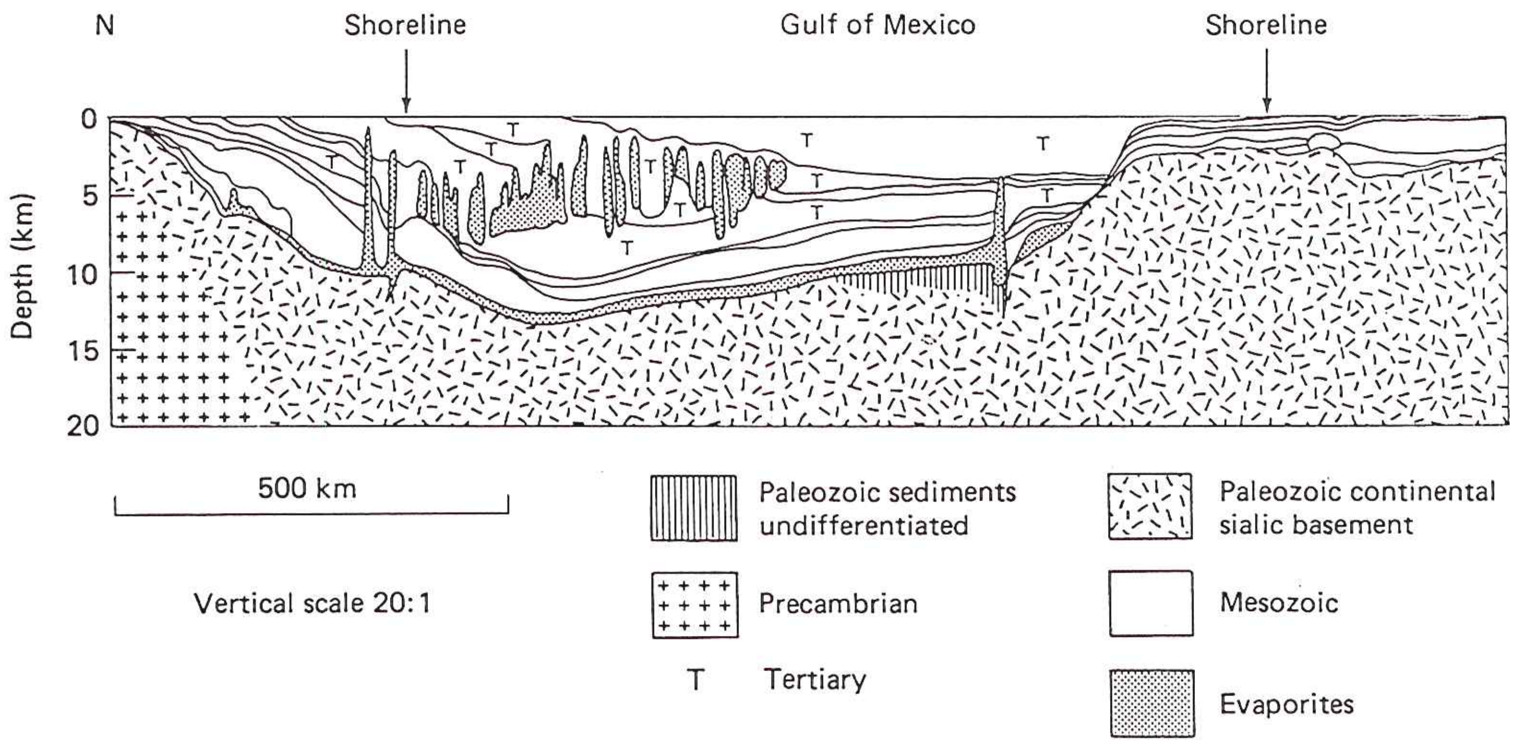

Figure 11-18 Geological cross section for the Gulf of Mexico. Vertical exaggeration is 20:1. (After Bally, 1979)

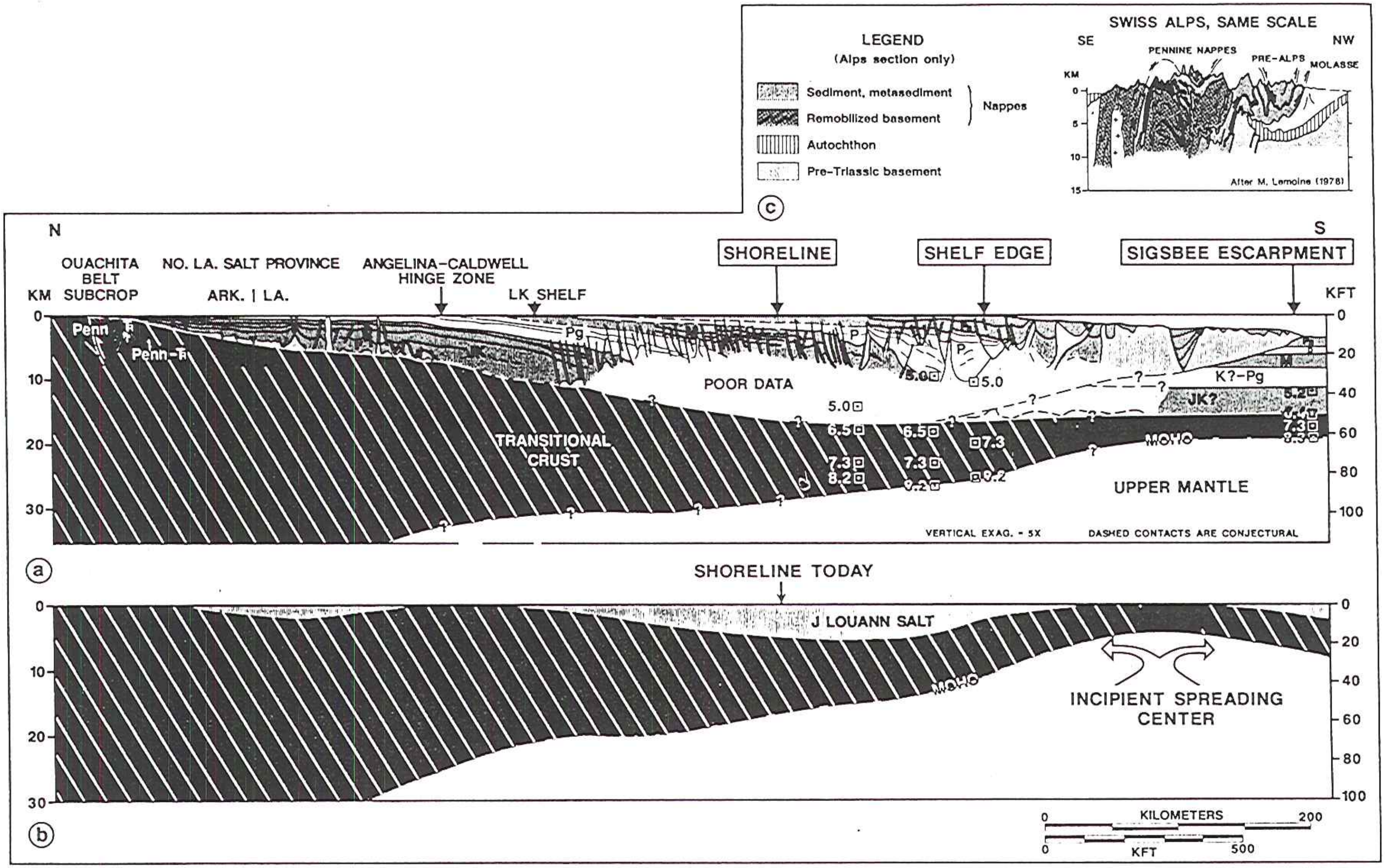

Figure 20. (a) North-south cross section, Louisiana; location on Figure 1. Vertical exaggeration = 5×. Dashed contacts highly conjectural. Northern half of section from A. D. Scardina (Shell Development Company, 1983). Refraction data in km/sec from Shell files. JK = Jurassic–Cretaceous; Pg = Paleogene; M = Miocene; P = Pliocene; Ps = Pleistocene. (b) Hypothetical reconstruction, mid-Jurassic time; (c) (upper right) Cross section of Swiss Alps after M. Lemoine (1978) drawn to same scale for comparison. The Sigsbee salt nappe is one of the largest structural features in North America and is apparently unique in scale if not structural style among the world's salt basins.

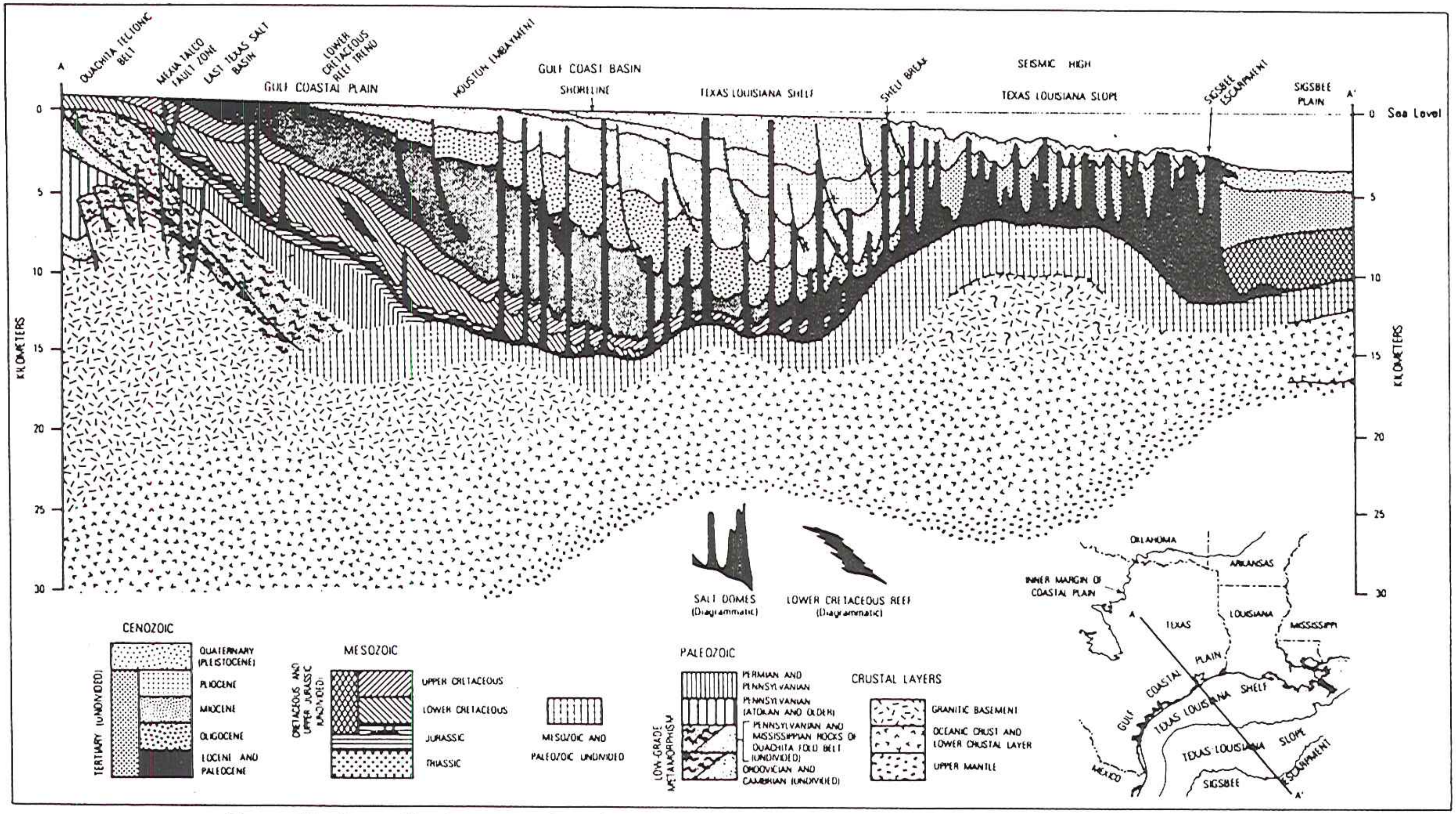

Figure 12. Generalized cross section of the northern Gulf of Mexico margin (from R. G. Martin, 1978, modified from earlier interpretations of Lehner, 1969; Dorman and others; 1972, Antoine and others, 1974; and Martin and Case, 1975).

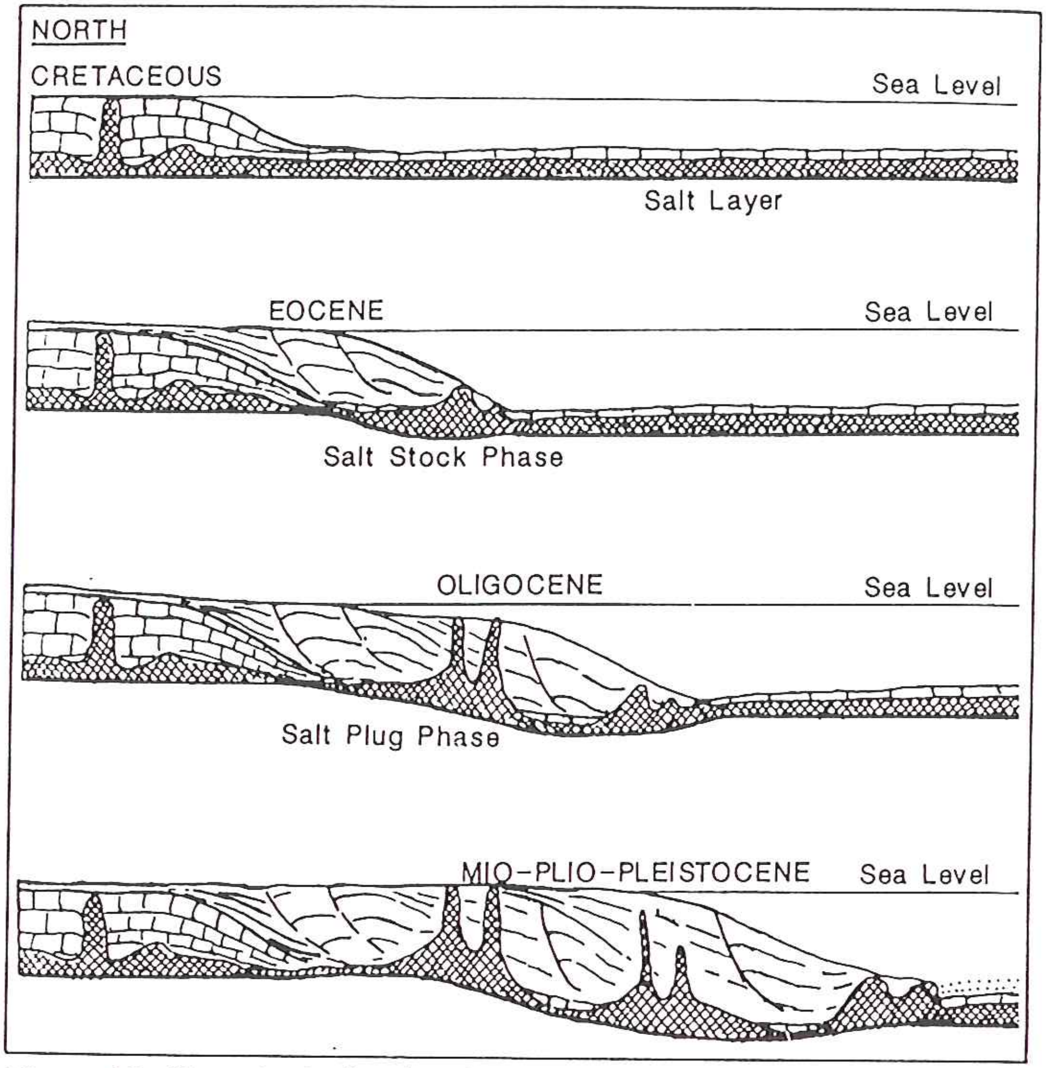

Figure 10. Hypothesis for the development of gravity-induced growth faults on a deep mobile salt layer, northern Gulf of Mexico (from Wilhelm and Ewing, 1972).

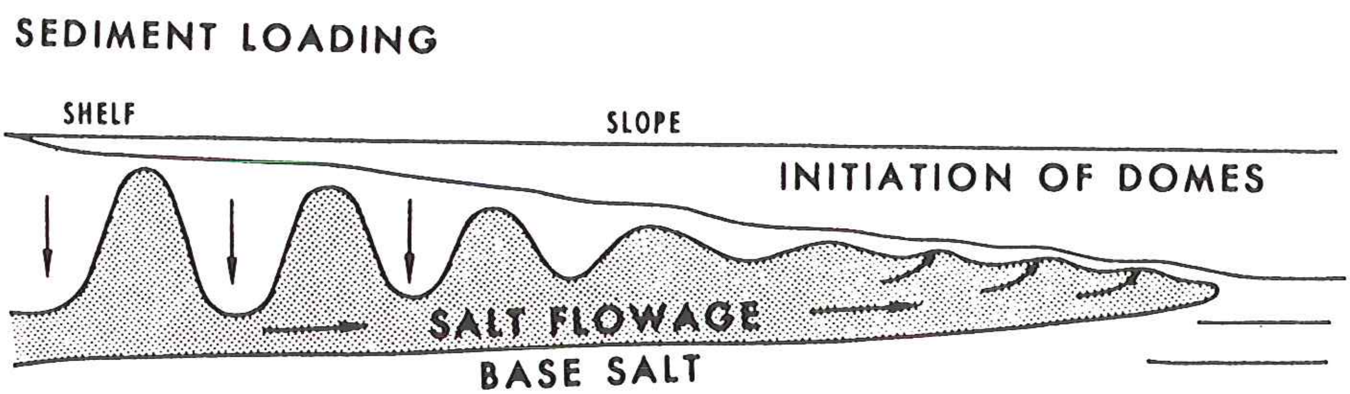

Figure 13. Diagrammatic representation of the initiation of salt dome growth on the continental slope as a result of sediment loading on the shelf–upper slope (from Humphris, 1978, 1979).

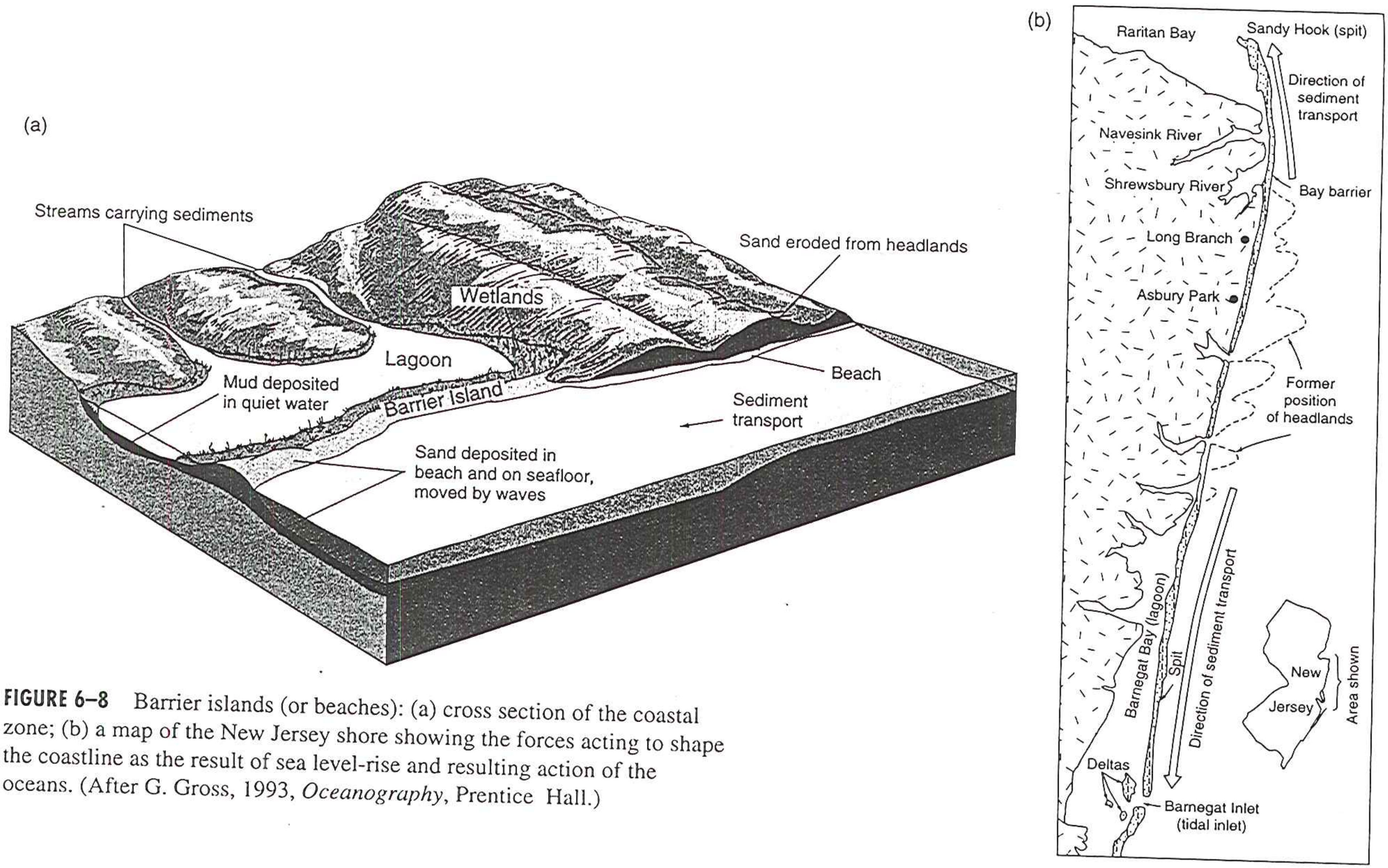

FIGURE 6–8 Barrier islands (or beaches): (a) cross section of the coastal zone; (b) a map of the New Jersey shore showing the forces acting to shape the coastline as the result of sea level-rise and resulting action of the oceans. (After G. Gross, 1993, *Oceanography*, Prentice Hall.)

5

Sediment Discharge from the Indus River to the Ocean: Past, Present and Future

J. D. MILLIMAN
Woods Hole Oceanographic Institution, Woods Hole, Massachusetts,
G.S. QURAISHEE
National Institute of Oceanography, Karachi,
and
M.A.A. BEG
Pakistan Council of Scientific and Industrial Research Laboratories, Karachi.

ABSTRACT

Until the late 1940's the Indus River apparently discharged more than 600mt of suspended sediment annually from the Himalaya Mountains. Assuming that most of the coarse fraction settled from suspension as the river flowed over the broad Indus Plain, somewhat less than 250mt reached the Indus delta annually. Since then, various man-made structures have greatly decreased the sediment load of the Indus. Today, less than 50mt reaches the estuary and, by the end of this decade, it may be practically nothing. To date, downstream barrages have accounted for most of the sediment decrease; dams have apparently only affected upper portions of the river basin. Such a dramatic drop in sediment and water flux can have serious impact upon the coastal environment.

INTRODUCTION

The Indus River is one of the world's largest rivers in terms of drainage area, river discharge and sediment load. Yet few people in Pakistan and far fewer in the western world know much detail about the water or sediment discharge from this river. Previous estimates of Indus sediment loads vary from 675 million tons (mt) before 1950 (WAPDA letter to G.S. Quraishee, December, 1982) to 435-440mt (Strahkov, 1961; Holeman, 1968) to 300mt (Kazmi, this volume). How these values relate to the actual amount of Indus sediment reaching the ocean depends upon where, when and how they were obtained (see e.g., Milliman and Meade, 1983). Now that the Indus is increasingly dammed and channeled, the applicability of these divergent values is particularly questionable; yet it is precisely at this time that an accurate understanding of the river is needed to predict possible impact upon the coastal areas from decreased sediment and water discharge.

In this paper we present a synthesis of available data from the Indus and also speculate on probable effects that damming will have upon the river and the adjacent marine environment. Several papers in this volume (e.g., Snedaker; Kazmi; Wells and Coleman; Schubel) deal with other aspects of the Indus, for which cross reference is recommended.

Most of our data are taken from the Pakistan Water and Power Development Authority (WAPDA), particularly data reports issued in 1975 and 1978, and as well as an unpublished report by the Civil Engineering Department of the Peshawar University (1970).

THE INDUS RIVER

The Indus drains the arid to semi-arid western Himalaya Mountains, with headwaters at elevations greater than 4000 m. The Indus and one of its tributaries (Sutlej River) are trans-Himalayan in origin, while the other main tributaries drain Afghanistan to the west (Kabul

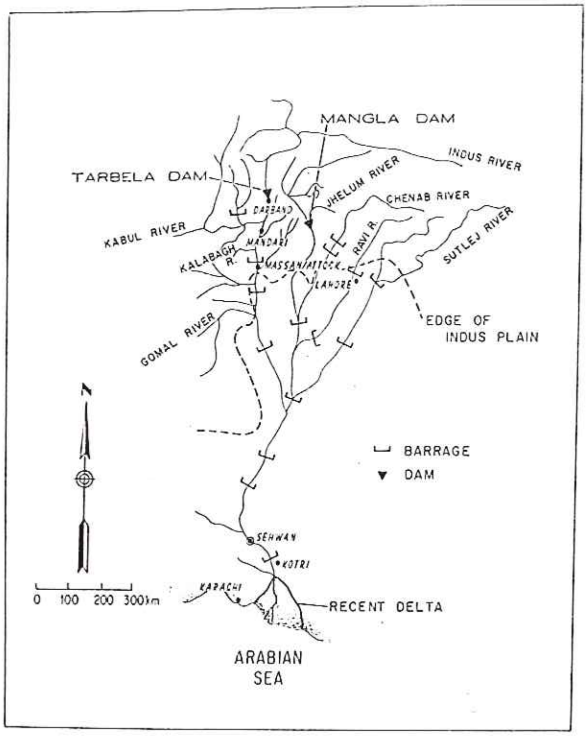

Figure 1. Map of Indus Basin, showing locations of barrages and dams.

River), and the southern side of the Himalayas (Jhelum, Chenab and Ravi rivers) to the east (Fig. 1). Upon leaving the mountains below Attock, the Indus River traverses across the broad Indus Plain for nearly 1000 km before reaching the Indian Ocean. Total drainage basin area is 970,000 km^2.

Although there is considerable variation in water flow between various stations in the river basin, flow is generally low in November to mid-spring, at which point snow melt (from the mountains) increases discharge. Highest discharge occurs in July, coincident with the peak of the rainy season. The six months, from May through October, account for more than 80 percent of the river discharge (Beg, 1977).

Quoted mean discharge for the Indus ranges from 5550 to 6700 to 7500 m^3 sec^{-1} (Lisitzin, 1972; Meybeck, 1967; UNESCO, 1978). WAPDA data for Sehwan, the most oceanward gauging station on the Indus, however, show that the mean for 1968-75 was 1810 m^3 sec^{-1}; upstream at Massan, flow during 1972-75 was 3440 m^3 sec^{-1}. During these times maximum discharge at the two stations was 18,200 and 22,300 m^3 sec^{-1}, respectively, while minimum discharges were 28 and 2000 m^3 sec^{-1} (WAPDA, 1977).

These numbers point to many of the problems inherent in discharging the Indus. One is that both discharge and sediment load change markedly in a downstream direction. Giving average discharge without quoting the station greatly hinders the applicability of the values. Moreover, as can be seen in Fig. 2, discharge varies greatly from year to year, meaning that short-term averages may or may not be indicative of longer-term discharge at a particular station. Finally, discharge has decreased dramatically since construction of dikes, channels, barrages and dams in the past 30 years. The discharge values first quoted (5550-7550 m^3 sec^{-1}) presumably represent upstream discharges for the years prior to wide-scale implementation of man-made structures along the river. In contrast, the smaller estimates are post-dam figures for the early 1970's; only half the water passing Massan reached Sehwan downstream, the rest being used for irrigation or lost to ground water aquifers (Beg, 1977). These average discharge values are even smaller at present with continued construction of dams and barrages.

Sediment Load of the Indus

Considerable amounts of sediment carried by the Indus come from glacially-derived material in the Himalayas as well as reworked fluvial deposits (Beg, 1977; van Aart, 1977). These unconsolidated materials plus the poor soil-holding capacity of the sparse vegetation (arid climate and geologically young terrain) result in large loads. As with water discharge, however, sediment loads vary so much in both time and distance along the river

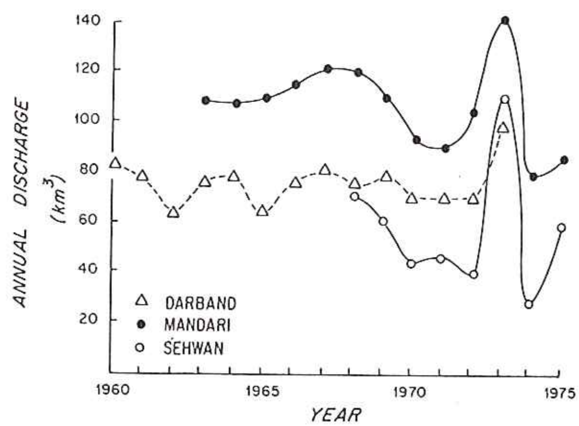

Figure 2. Annual discharge values for Darband, Mandari and Sehwan (see Figure 1 for locations). Data from WAPDA (1979).

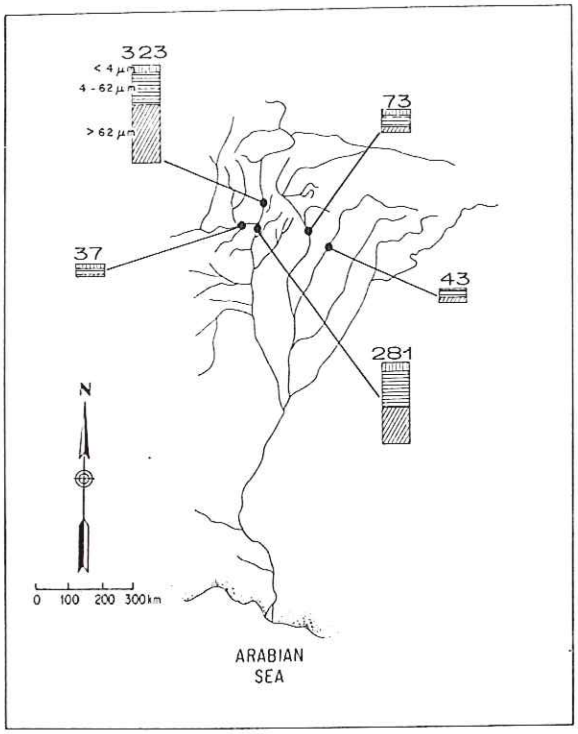

Figure 3. Size distribution of average sediment load on the Indus and tributaries 1960-68. Data from Peshawar University, 1970.

that previously quoted values are more or less meaningless. Even values quoted for the same station and the same year disagree between reports, presumably because of different sediment-rating curves used. For example, Peshawar University estimated sediment discharge at Darband in 1966 to be 347 mt, while WAPDA, using the same raw data, calculated a load of 295 mt.

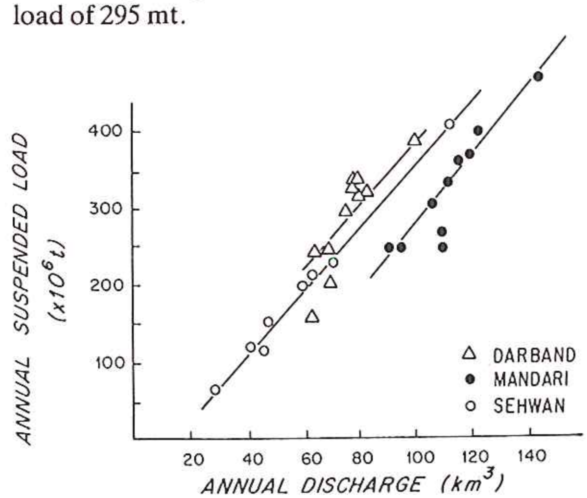

Figure 4. Comparison of annual discharge and sediment loads for the Indus for stations at Darband, Mandari and Sehwan. Data from WAPDA (1979).

Using, for the time being, the Peshawar University figures, between 1960 and 1968 more sediment passed Darband (since covered by the lake created by the Tarbela Dam) than passed Mandari downstream (Fig. 3). Combining the 37 mt entering from the Kabul River with the Indus load, an estimated 80 mt of sediment settled out from the Indus annually between Darband and Mandari. The settled sediment appears to be primarily sand-size material, presumably deposited along this relatively flat valley floor. The decreased competence of Indus River water at Mandari is seen by a lower annual rating curve (i.e., higher discharge required to maintain an equal load to that at Darband—Fig. 4). WAPDA sediment load values show that the load at Mandari can be either greater or lower than that at Darband, depending upon the year (see Fig. 5). Whether these or the Peshawar values are more realistic has not been resolved at this time.

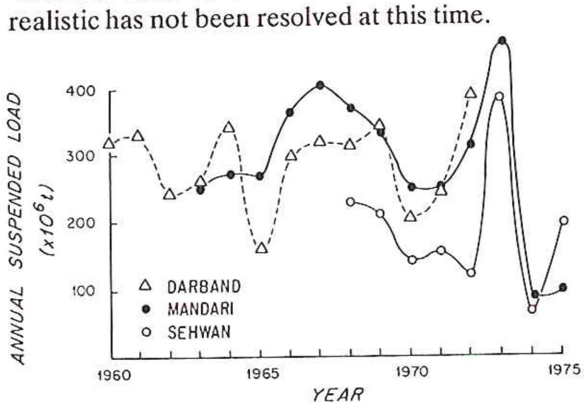

Figure 5. Yearly variation in suspended load passing Darband, Mandari and Sehwan; Darband observations were discontinued in 1973 with the completion of the Tarbela Dam. Data from WAPDA (1979).

To summarize the natural system, much of the Indus sediment load comes from the upper reaches of the drainage basin which, because of the close proximity to the mountains, means a substantial percentage of sand (60 percent at Darband; Fig. 3). Some of this sediment settles downstream of Darband as the river flattens into a relatively low-gradient valley. Below Mandari the gradient increases and a number of large tributary rivers empty into the Indus, increasing the sediment load. As the river begins to flow across the Indus Plain, however, coarse sediment again settles out; by Sehwan, still some 300 km from the sea, 20 to 50 percent of the total load has been lost. Kazmi (this volume) reports much of the present river valley is underlain by more than 100 m of late Quaternary sediment, and McDonald (1966, in

Peshawar Univ., 1970) estimated a vertical accretion in the flood plain of 9 m in the past 5000 years and a seaward growth of the delta of 80 km in 2000 years. Thus, it is not difficult to conclude that a large portion of the suspended load in the Indus is deposited prior to reaching the ocean. If the sand constitutes 60 percent of the load at Darband, then perhaps 60 percent or more of the total load may be deposited over the flood plain.

Man's Influence on Sediment Discharge

Before the 1950's the discussion presented in the previous sections was probably a fairly representative of Indus discharge patterns. Since then, however, human activities have greatly altered discharge patterns of the Indus and, therefore, transport of sediment. Four general types of engineering activities have occurred along the Indus; 1) channels which transfer water to and from various river branches as well as to irrigate farmland; 2) barrages which aid river control by diverting river flow to channels; 3) embankments and dikes which prevent river overflow, thereby restricting flow to the main channels; and 4) dams which are used for hydroelectric power, irrigation and flood control.

Wide-scale alteration of the Indus began in the 1940's with construction of barrages and channels. Prior to this time, annual sediment discharge (at Darband or Mandari ?) may have been the 675 mt quoted above. Assuming that at least 60 percent (sand) plus some of the finer load was deposited along the flood plain, less than 250 mt should have reached the Indus estuary. Neither the source nor the years of the values of 435-440 mt quoted by Lisitzin and Holeman (the latter taken from Fornier, 1960) is clear, but we assume that these may represent sediment discharge at Darband or Mandari in the 1950's. The difference between these and earlier estimates, therefore, would represent the sediment lost to the river system from channels and barrages. The effect of barrages on river flow can be seen at Kotri, 200 km from the sea, where Indus discharge during autumn, winter and early spring months was practically eliminated after barrage construction (used for irrigation during these dry months) and flow during summer months was only high during periodic peak flow (Fig. 6).

Embankments and levees have been utilized since British occupation. While they have helped control flooding of vast areas of the Indus flood

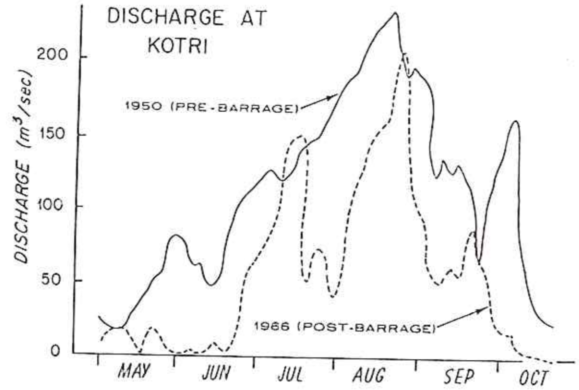

Figure 6. Comparison of discharge values at Kotri before and after barrage construction. Data from WAPDA (1979).

plain, they also have increased salinities in ground waters (Beg, 1977). Moreover, by not allowing suspended sediment to settle over the surrounding flood plain, much of the coarser load has settled on to the river bed, thus progressively elevating the river bed relative to the flood plain. It is not clear how (or if) the embankments have actually altered total sediment discharge from (or along) the Indus.

Two huge dams were constructed on the Indus system and have been operating for the past 10-15 years. Each has had a major impact upon sediment load. The Mangla, damming the Jhelum River, was completed in 1967. Soon after completion, the sediment load of this river fell from an average of 45 mt to less than 0.5 mt (WAPDA, 1978). Down-dam erosion of river banks and the channel presumably restored some of the Jhelum load. The Tarbela Dam, on the Indus near Darband, was completed in 1974. Sediment loads downstream decreased sharply in both 1974 and 75, the last two years for which we have records. At Mandari, loads averaged less than 100 mt compared to the previous three years when loads averaged more than 300 mt (Fig. 5). At Sehwan, sediment loads were somewhat greater than at Mandari, suggesting net erosion of the river channel/banks, and, therefore, little to no net accumulation along the intervention flood plain and river system.

Future of the Indus River System and Estuary

Although the actual sediment load reaching the Indus estuary has not been documented in the past and is not known today, it is safe to assume that as recently as 30 years ago perhaps somewhat less than 250 mt of sediment may have reached the estuary annually. As of 1974-75, this amount was down to less than 100 mt. Presumably it is even less today, and within the next 10 years further construction along the Indus may completely cut off sediment supply reaching the ocean. Effects of this diversion are considerable and should increase in the future.

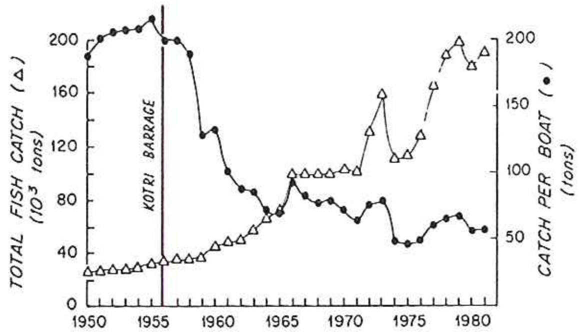

Figure 7. Yearly variations of total fish catch and fish catch per boat along the Sind coast. Construction of the Kotri barrage is shown in 1955. Modified from Quraishee (1975).

Channel and embankment construction have resulted in increased salinities in ground waters, often, negating the positive aspects associated with irrigation. The decreased amount of river flow also has increased salinities in the Indus estuary, thereby killing or hindering mangrove communities, a point dealt with by Snedaker in this volume. Finally, the decreased influx of nutrient-rich river waters, undoubtedly, will affect offshore fisheries. Yearly catches of fish off the Sind Coast increased 7-fold between 1950 and 1981, but becuase of a 23-fold increase in the effective number of fishing boats in this area, the actual catch per boat fell by nearly 3½-fold (Fig. 7). This decrease might be explained by the increased number of boats, catching a more or less constant supply of fish, but the decrease in catch per boat occurred with the construction of the Kotri Barrage in 1955, several years before the number of boats increased substantially. This suggests that decreased river discharge across the barrage may have played a role in the decreased yield (Quraishee, 1975).

Upstream construction of dams on other large rivers also prevented suspended sediment from reaching the ocean, most notably the Colorado and Nile Rivers, both of which had annual loads of 100 mt or more. The Indus, however, is by far the largest such river to be dammed, and also has a very high energy coastline and shelf (Wells and Coleman, this volume). Thus, cutting off the large sediment load has particularly great potential for high coastal erosion of the Indus delta. The papers by Schubel and by Wells and Coleman in this volume deal with this problem further.

Note of Additional Evidence

Subsequent to the preparation of this manuscript, one of us (G.S.Q.) obtained a nearly 50-year record of annual discharge and suspended load for the Indus at Kotri, about 250 km upstream from the river mouth. This particularly long record substantiates many of our other data and speculations, and also answers many questions (Fig. 8). Aside from the marked annual variations, three distinct periods are noted in the Kotri records:

1) From 1931 through 1947, discharge generally averaged or exceeded 90 km³/yr, and suspended load exceeded 200 mt. The average for the 17 years prior to 1948 was 225 mt, in reasonable agreement with our previous estimates for the years prior to the late 1940's.

2) From 1948 through 1961, the river was in transition, with continued high discharge but decreasing suspended loads. The measured Indus load at Kotri, for example, fell from 275 mt in 1945 to less than 50 mt in 1948. Other than two years of high loads in 1955-56, the suspended load during this transition period was generally substantially less than 100 mt. Water discharge, however, remained high (Fig. 8). This change in river character probably resulted from construction of

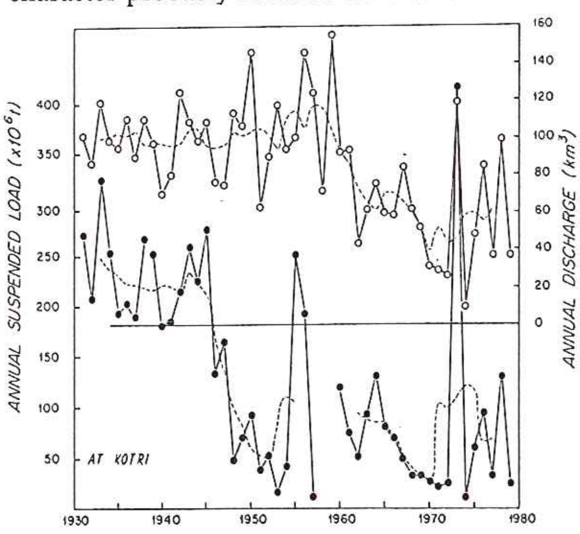

Figure 8. Discharge and sediment loads for the Indus River at Kotri, 1931-1979. Dashed lines represent 5-yr running mean averages. Data from the Indus River Commission.

one or more barrages along the lower course of the river.

3) After 1961, discharge dropped dramatically whereas discharge in the 1950's exceeded 100 km^3/yr, it often was less than 60 km^3/yr in the 1960's and 70's (Fig. 8). Suspended load dropped slightly, but major yearly fluctuations continued (particularly in the 1970's). As this drop in discharge and the previous drop in sediment load occurred before construction of upstream dams, we assume they resulted from continued barrage construction and corresponding irrigation of the river.

One further indication of change in the river can be seen in the marked change in rating curves for the Indus during these three periods (Fig. 9), with highest competency prior to 1948, and lowest during the transition period (1947-60). The trend of pre-1948 curve parallels and is closest to the Sehwan curve, inferring an approximate continuum with the upstream portion of the river. The strong disparity between the other two curves and the Sehwan curve, however, suggests that the downstream character of the Indus changed before the upstream (1948 versus 1974). Dam construction appears to have strongly altered the carrying capacity of the upper Indus, whereas it appears to have had little impact in the lower Indus, as indicated by the continuity of post '61 Kotri data (Fig. 9). Barrage and irrigation construction presumably was more important in decreasing flow and sediment load in the lower river. Other than the unusually high sediment load in 1976, an average of less than 50 mt was carried past Kotri annually. Presumably the amount presently reaching the ocean in the mid-1980's is even less.

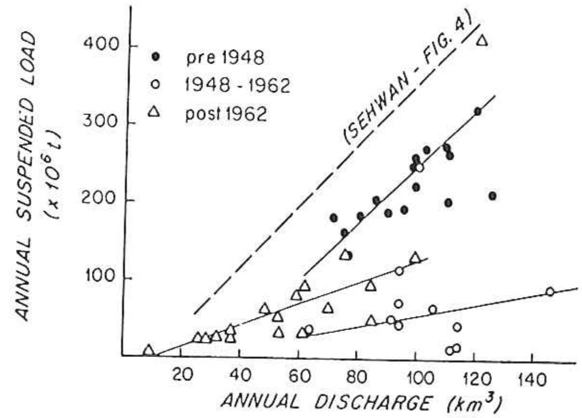

Figure 9. Sediment rating curve at Kotri. Note the marked difference in trends for the 3 periods represented in the 49 year record (Fig. 8). For reference, the Sehwan trend (from Fig. 4). is also shown.

ACKNOWLEDGMENTS

We thank the National Science Foundation for sponsoring the Pakistani workshop that allowed us to discuss this paper. Partial funding for the senior author was from the Office of Naval Research (Contract No. N00014—8IC—0009). We thank Drs. David Aubrey (WHOI) and Bilal Haq (EXXON) for reviewing this paper. This is Wood Hole Oceanographic Institution Contribution Number 5486.

REFERENCES

Beg, M.A.A., 1977. The Indus River basin and risk assessment of the irrigation system. Int. Working Seminar on Environmental Risk Assessment in an International Context. Tihanyi, Hungary, 13 p.

Holeman, J.N., 1968. Sediment yield of major rivers of the world. Water Resources Red., 4: 737-747.

Lisitzin, A.P., 1972. Sedimentation in the world ocean. Soc. Econ. Paleont. Mineral. Spec. Publ., 17: 218 p.

Meybeck, M., 1976. Total mineral dissolved transport by world major rivers. Bull. Sci. Hydrol., 21: 265-284.

Milliman, J.D. and R.H. Meade, 1983. Worldwide delivery of river sediment to the oceans. J. Geol., 91: 1-21.

Pakistan Water and Power Development Authority (WAPDA), 1975. Sediment Appraisal of West Pakistan Rivers, 1960-1972. Surface Water Hydrology Project, Lahore.

Pakistan Water and Power Development Authority (WAPDA), 1978. Sediment Appraisal of West Pakistan Rivers, 1960-1972. Surface Water Hydrology Project, Lahore.

Peshawar University, 1970. The sediment load and measurements for their control in rivers of West Pakistan. Peshawar Univ. Civil Eng. Dept., Water Res. Div., 1: 214 p.; 2: 320 p.

Quraishee, G.S., 1975. Influence of the Indus River on marine environment. Int. Conf. Management of Environment. Pakistan Acad. Sci., Islamabad, p. 111-122.

Strahkov, N.M., 1961. Onekotroykh zakonomernostiakh denudatsii in perenosa osadochnogog materiala na ploschadyakh gymidnykh klimatov, *In:* N.M. Strahkov, P.L. Bezrykov, and V.S. Yablokov (eds.), *Sovremennye osadki moei i oceanov*. Moscow, Izdatelstove Akademia Nauk SSSR, p. 5-27.

van Aart, R., 1977. The Indus Delta. ILRI, Netherlands, unpubl. rept.